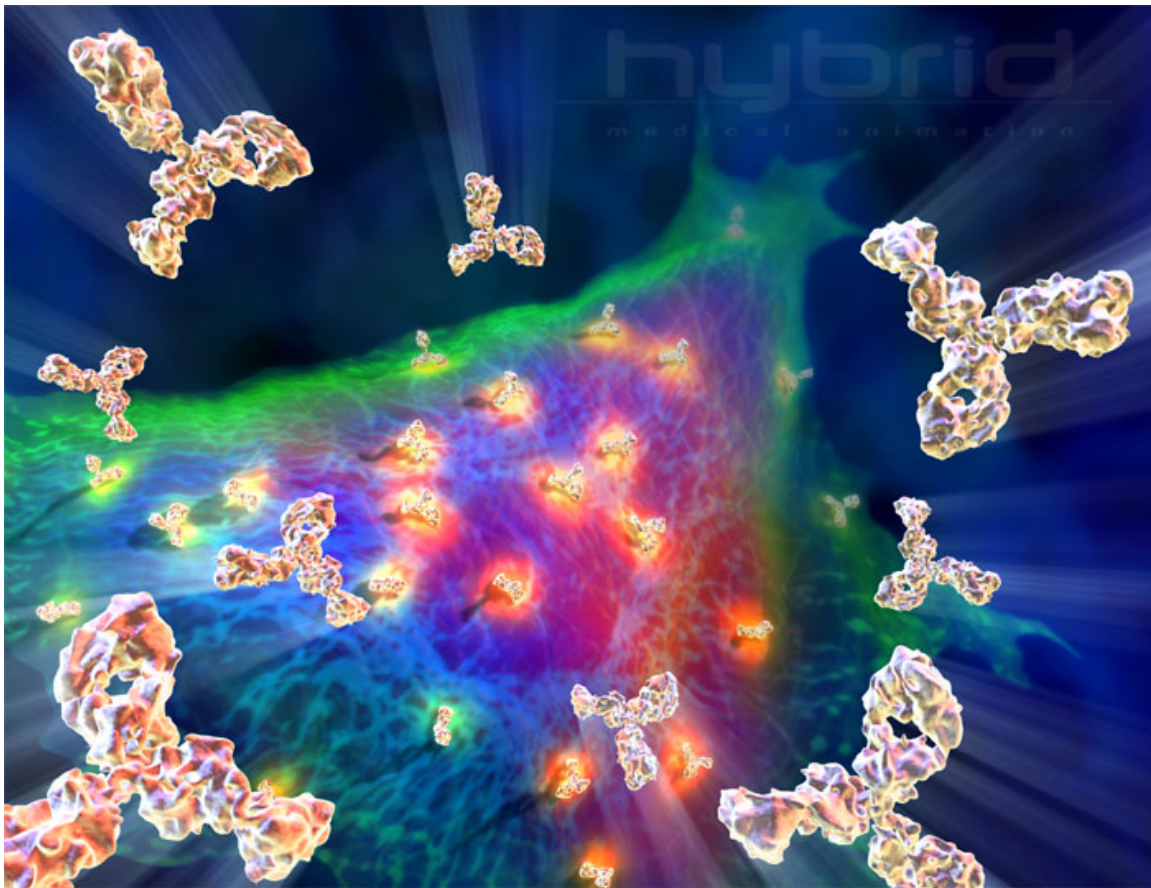

**CCKK DRUG DELIVERY TECHNOLOGIES:
MONOCLONAL ANTIBODIES FOR DELIVERY OF
CHEMOTHERAPY DRUGS FOR CANCER THERAPY**

Technical Report and Business Plan



April 29, 2005

Submitted to Dr. Miguel Bagajewicz

Submitted by:

Sarah Clawson

Paul Cole

Sarah Katen

Nell Keith

Table of Contents

| | |
|---|-----------|
| 1. Abstract | 5 |
| 2. Introduction | 6 |
| 2.1 Malignant Tumors: Gliomas | 7 |
| 2.2 Blood Brain Barrier | 8 |
| 2.3 MAb 81C6 | 9 |
| 3. Existing Treatment Options | 10 |
| 3.1 Antibody alone | 10 |
| 3.2 Antibody with Toxin | 11 |
| 3.3 MAb conjugated to radionuclide | 12 |
| 4. Proposed Alternative Treatment Methods | 13 |
| 4.1 Immunomicelles | 13 |
| 4.2 Vector Mediated Transcytosis | 14 |
| 4.3 Immunoliposome | 16 |
| 4.4 Immunoliposomes vs. Immunomicelles | 16 |
| 4.5 Nanoparticles | 17 |
| 4.6 Chemotherapy Toxin Choices | 18 |
| 4.7 Temodar Product Information | 19 |
| 5. Production of Monoclonal Antibodies | 20 |
| 5.1 Laboratory Scale Production/Isolation of Monoclonal Antibodies | 20 |
| 5.2 Large Scale Production of MAbs | 22 |
| 6. Immunomicelle Production and Drug Encapsulation | 26 |
| 6.1 Production of Immunomicelle | 26 |
| 6.2 Immunomicelle with Temodar[®] | 27 |
| 7. Treatment | 28 |
| 7.1 Blood Supply to the Brain | 28 |
| 7.2 Blood Temodar[®] Concentration Model | 29 |
| 7.3 Drug Delivery by Injection as a Function of Tumor Volume | 32 |
| 7.4 Brain Immunomicelle Concentration Model | 36 |
| 8. Animal Testing | 41 |
| 9. Business Plan | 41 |
| 9.1 Business Goals and Market Strategy | 41 |
| 9.2 Business Organization | 43 |
| 9.3 Glioma Incidence in the US | 45 |

| | |
|---|------------------|
| 9.4 Plant Location | 46 |
| 9.5 Funding | 49 |
| 9.6 Cost | 50 |
| 9.7 Pre-FDA Testing | 51 |
| 9.8 FDA Testing and Approval | 56 |
| 9.9 Marketing | 58 |
| 9.10 Economic Demand Model..... | 59 |
| 9.11 Risk Analysis | 63 |
| <i>10. Conclusions</i> | <i>77</i> |
| <i>11. References</i> | <i>78</i> |
| <i>A1. Appendix 1</i> | <i>81</i> |
| A1.1 Nanoparticles | 81 |
| A1.2 Production of Nanoparticles..... | 82 |
| A1.3 Problems with Nanoparticle Treatment..... | 82 |
| A1.4 Pre-FDA Testing of Nanoshell Delivery Mechanism | 85 |
| <i>A2. Appendix 2</i> | <i>87</i> |
| A2.1 Pharmacokinetic Parameter Derivation | 87 |
| <i>A3. Appendix 3</i> | <i>91</i> |
| A3.1 NPV Distributions of Each Successful Scenario | 91 |

Table of Figures

| | |
|---|----|
| Figure 1: Monoclonal Antibodies Binding to Epitopes | 6 |
| Figure 2: Malignant Glioma | 7 |
| Figure 3: Blood Brain Barrier Illustration | 9 |
| Figure 4: Antibody Treatment Mechanisms | 11 |
| Figure 5: Cross-sectional View of a Micelle | 13 |
| Figure 6: Vector Mediated Transcytosis | 15 |
| Figure 7: Cross-sectional View of a Liposome | 16 |
| Figure 8: Electron Micrograph of Nanoparticles | 18 |
| Figure 9: Temodar [®] Molecular Structure | 20 |
| Figure 10: MAb Isolation Technique | 21 |
| Figure 11: Process Flow Diagram for Monoclonal Antibody Production Plant | 25 |
| Figure 12: MAb-Micelle Attachment Reaction | 27 |
| Figure 13: Vascular Network of the Brain | 29 |
| Figure 14: Micelle and Temodar [®] Oral Dosage Elimination Model | 32 |
| Figure 15: Common Carotid Artery Branching | 33 |
| Figure 16: Drug Delivery Standard Curve | 35 |
| Figure 17: Two Compartment Model | 36 |
| Figure 18: Equilibrium Elimination Model | 37 |
| Figure 19: Redistribution Phase Equilibration Model | 38 |
| Figure 20: Micelle Two Phase Elimination Model | 40 |
| Figure 21: Sales of Monoclonal Antibodies for Cancer | 43 |
| Figure 22: Population Growth of the United States | 46 |
| Figure 23: Location of Top 50 Cancer Treatment Centers in the US | 48 |
| Figure 24: Pre-FDA Possibilities | 51 |
| Figure 25: Pre-FDA Micelle Testing Flow Chart | 54 |
| Figure 26: Pre-FDA Micelle Testing Pathways | 55 |
| Figure 27: FDA Approval Pathways | 57 |
| Figure 28: α Function Model | 62 |
| Figure 29: NPV Risk Curve for Minimal R&D Spending | 71 |
| Figure 30: Risk Curves for Varying First-Stage Decisions | 72 |
| Figure 31: NPV Distribution at 5 Years of Most Probable Success | 73 |
| Figure 32: NPV Distributions for Successful Pathways | 74 |
| Figure 33: Module 1 NPV Distribution | 75 |
| Figure 34: Module 2 NPV Distribution | 76 |
| Figure 35: Module 3 NPV Distribution | 76 |
| Figure 36: Module 4 NPV Distribution | 77 |
| Figure 37: Structure of Polybutylcyanoacrylate | 84 |
| Figure 38: Pre-FDA Testing of Nanoshell Flowchart | 86 |
| Figure 39: Two Compartment Model Diagram | 87 |

Table of Tables

| | |
|---|----|
| Table 1: Pharmacokinetic Parameters | 39 |
| Table 2: Available Funding from NIH | 49 |
| Table 3: Pre-FDA Pathway Probabilities | 65 |
| Table 4: FDA Approval Process Probabilities | 66 |
| Table 5: FDA Approval Process Probabilities | 67 |
| Table 6: FDA Approval Process Probabilities | 68 |
| Table 7: FDA Approval Process Probabilities | 69 |

1. Abstract

Malignant Gliomas affect six to nine thousand Americans every year: the average survival time for a patient with this disease is 40 to 60 weeks. CCKK Drug Delivery Technologies has developed a treatment utilizing monoclonal antibodies (MAbs) to selectively deliver a chemotherapy drug directly to the tumor cells. The MAb used, 81C6, targets tenascin, which is in the extracellular matrix of the tumor. The antibody will be attached to a micelle and the toxin will be encapsulated within the micelle. This method will increase the damage to the tumor cells while decreasing the damage to the rest of the body.

CCKK Drug Delivery Technologies will be a drug delivery technology company that will solicit other, larger drug companies to partner in the use of their drug with our immunomicelle technology. Company expenditures will be focused primarily on developing the delivery of the toxin to the cancer cell. Doing this will decrease our FDA costs because the drug manufacturer will absorb the majority of the costs.

The production facilities will be located in the Boswash, a megalopolis which runs from Boston south west to Washington DC, including Philadelphia, New York City, and Hartford, as well as all surrounding suburbs, in order to utilize the expertise and resources afforded by three of the top five cancer facilities in the U.S. as well as those of top research universities. Pre-FDA testing will be done at Johns Hopkins, Yale, or Harvard in order to employ their expertise and take advantage of available NIH funding for university research; the NIH is the major funding source for research in cancer therapy, especially at the university level. The average amount of NIH grants that can be obtained by building in this area is approximately \$3,789,000. It is estimated that the pre-FDA testing will cost between \$2.5 million and \$4.5 million and last thirteen years if the project is to advance to FDA testing. Therefore, obtaining these grants is critical to the financial feasibility of the project.

The facilities costs were estimated at \$31.5 million, including facilities for antibody, vector, and micelle production, as well as a pre-FDA research facility. The facilities for commercial production will be built during stage II of FDA testing, assuming the treatment passes all of the previous stages.

FDA trials will be conducted to determine the safety, short term side effects, and long term side effects of the treatment. FDA testing will require approximately \$20 million to fund the participating doctors' salary and patients' treatment for a duration of approximately 21.5 years.

The treatment cost per patient is set as \$15,000 per year. This price allows for recovery of the capital investment in three years with a significant profit margin. The three years begins once FDA approval is granted and production has begun. A final NPV of the most likely scenario is around \$100 million.

2. Introduction

Antibodies are proteins produced by the plasma cells in the immune system in response to antigens, or foreign substances to the body that could possibly be detrimental to the cell. Antibody-antigen complexes initiate a cascade of protective reactions in cells of the immune system. Monoclonal antibodies are Y-shaped proteins with an antigen binding region located at the end of each arm. According Charles A. Janeway and colleagues in the book Immunobiology, a monoclonal antibody is an antibody that binds to a single epitope. In cancer cells, an epitope is often a protein on the cancer cell's surface, as shown in the following figure.¹

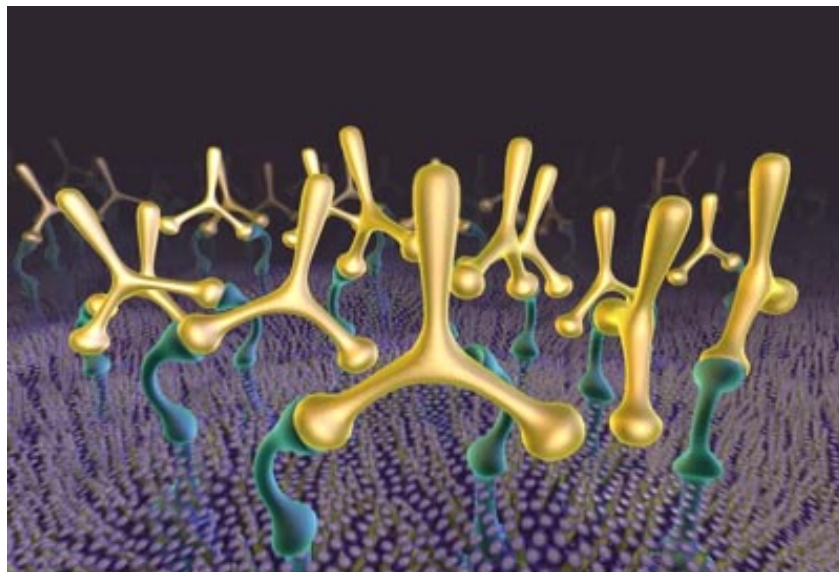


Figure 1: Monoclonal Antibodies Binding to Epitopes

<http://www.strayvr.com/FullyHuman.jpg>

Monoclonal antibodies (MAbs) can be linked to toxins or radioactive compounds to be used as various treatments for diseases. Because MAbs are specific to a single epitope, they will bind only to the cell being targeted. When choosing a MAb for treatment, it is important to pick a MAb that will bind only to the antigen or cancer cell, minimizing binding to other sites within the body. When using an attachment, the cell can either be

killed by radiation from the molecule attached to the MAb or by the release of the toxin in the cell after it engulfs the antibody.¹

2.1 Malignant Tumors: Gliomas

Malignant gliomas are the most common type of brain cancer in adults. Gliomas are divided into two categories: anaplastic astrocytoma (grade III) and glioblastoma multiforme (grade IV). Glioblastoma multiforme (GBM) is the faster growing and most common of the two. According to Dr. Glen Stevens from the Cleveland Clinic, malignant gliomas affect two to three people per 100,000 people every year.² This translates to approximately six to nine thousand Americans every year. Even with existing treatment, the average survival time is a mere 40 to 60 weeks, according to Dr. Ilkcan Cokgor, a scientist studying gliomas treatment.³

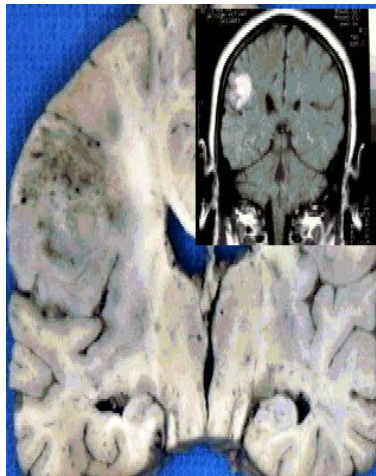


Figure 2: Malignant Glioma

<http://www.tumorboard.com/tumorboard/images/gbmc.jpg>

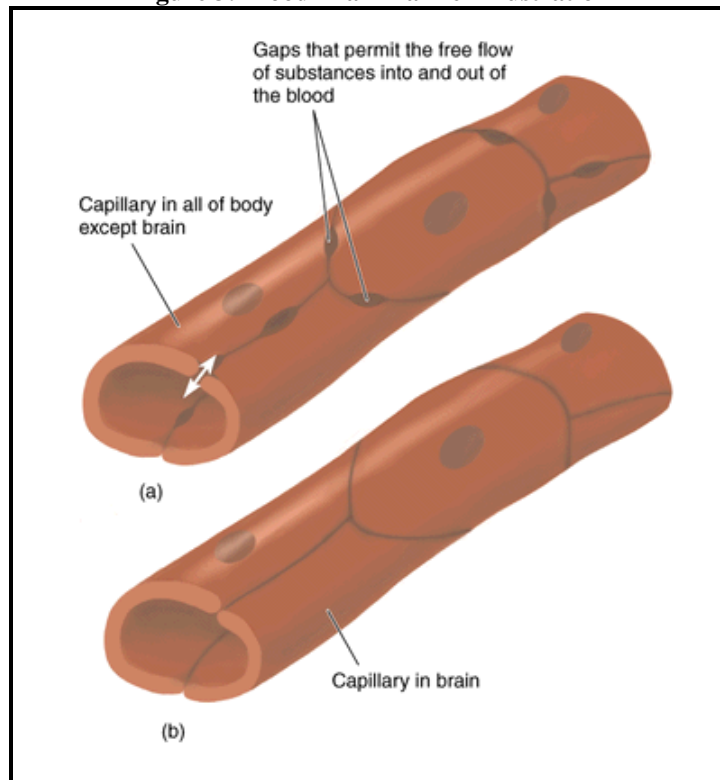
According to the American Tumor Association, traditional treatments for gliomas include surgery, chemotherapy, and radiation, which are often done in combination. However, surgical removal of the tumor is not always a viable option for patients, as the tumor may be located in close proximity to major arteries or neurologically sensitive areas in the

brain. The goal in tumor removal is to eliminate the tumor without causing severe neurological damage. Partial removal of the tumor will also help alleviate symptoms by reducing the relative size of the tumor, which will result in a decrease the intracranial pressure, thereby relieving the symptoms associated with this disease. Traditional radiation utilizes either X-rays or gamma rays aimed at the tumor to disrupt the tumor growth. Chemotherapy agents target and kill rapidly growing cells; they can be used before or after surgery and during radiation therapy.⁴

2.2 Blood Brain Barrier

The blood-brain barrier (BBB) is present to protect brain cells from harmful, foreign molecules. It manifests itself in the form of tight junctions in brain capillary endothelial cells that prevent molecules from entering glial cells (brain tissue). As seen in Figure 2, the gaps present in capillaries in the rest of the body do not occur in the capillaries in the brain. According to Dale Purves and colleagues in the book Neuroscience, entry can be achieved only by a molecule's high solubility in lipids or by a transporter mechanism.⁵ If a molecule is lipid insoluble and not normally transported across the blood brain barrier, the molecule can be transported by attaching it to a vector according to Dr. WM Pardridge from the UCLA School of Medicine. The vector can be a modified protein or an antibody, but the vector must normally predisposed to crossing the BBB.⁶

Figure 3: Blood Brain Barrier Illustration



<http://homepage.psy.utexas.edu/homepage/class/Psy332/Salinas/Cells/BBB.gif>

2.3 MAb 81C6

Tenascin, a surface protein, is produced by gliomas; the only location of this protein in the brain is in glioma cells. 81C6 is a MAb produced in response to this protein. The residence time of 81C6 has been tested and determined to be 79 hours in the tumor and 36 hours in the rest of the body.³ The binding of the antibody is a reversible reaction, and the antibody continually binds to and dissociates from the receptor. Therefore, since the concentration of binding sites is higher in the tumor, the antibodies that dissociate have many more receptors to which they can rebind.

Tenascin is also found in other parts of the body in relatively small amounts, especially connective tissue and developing organs including kidneys, mammary glands, and the

teeth. Unwanted binding of the MAb to tenascin in these locations could cause harmful side effects. However, according to Chiquet-Ehrismann, the most abundant source of tenascin found in the body is in glioma cells.⁷ Therefore, if MAb 81C6 is used to deliver treatment, the effects on the other parts of the body containing tenascin are relatively small compared to the tumor cells.

3. Existing Treatment Options

3.1 Antibody alone

One treatment option utilizing monoclonal antibodies (MAbs) involves using only the antibody, which can initiate the immune response of natural killer cells (NK). The treatment would include the intake of tumor-specific antibodies targeting tumor-specific antigens found on the tumor cell surface followed by a natural immune response. There are currently treatments for breast cancer and non-Hodgkin's B-cell lymphoma utilizing this technology that are already FDA approved. These treatments are done in conjunction with chemotherapy surgery, and/or radiation. The humanized form of MAb used to treat breast cancer is known as Herceptin, which targets a growth hormone that is over-expressed in approximately $\frac{1}{4}$ of breast cancer patients.

One problem with this MAb treatment in cancer is the genetic instability of some cancer cells; the phenotypes of the cancer cells are constantly changing, and thus it is difficult to maintain a treatment regime based on cell specificity. The first successful treatment using MAb without a ligand was in B-cell lymphomas. After treatment the tumor usually

went into remission, but later reappeared. When the tumor manifested a second time and was re-treated, the MAb was no longer able to bind to the tumor cell surface. Also, inefficient killing of the tumor cells by the immune system presents another problem with the use of MAb treatment without the use of a ligand; if the tumor is not entirely killed, remaining cells can continue to divide and cause the tumor to reappear.¹

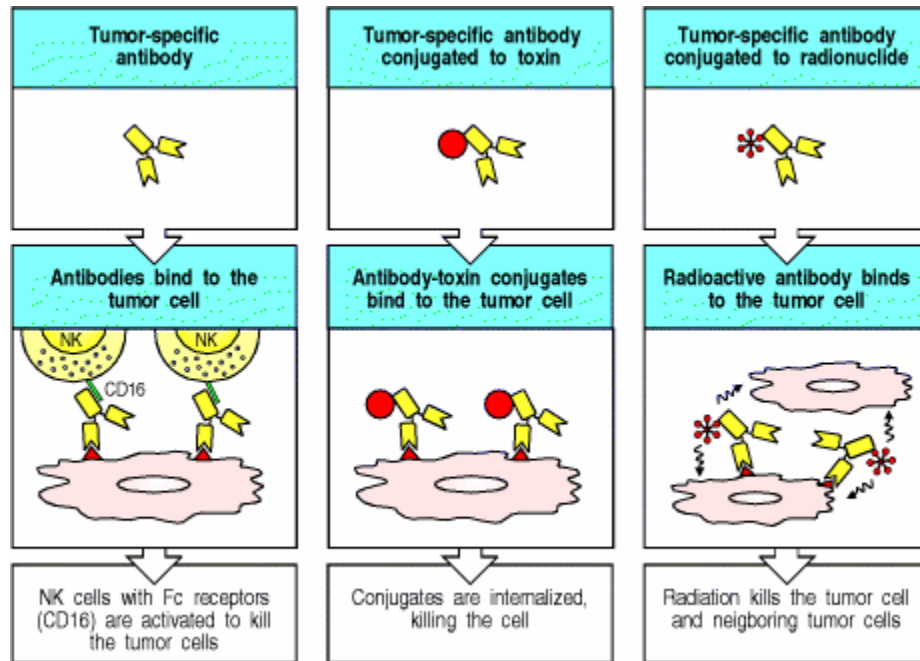


Figure 4: Antibody Treatment Mechanisms

3.2 Antibody with Toxin

Attaching a toxin to the MAb, forming a complex known as an immunotoxin, is one way to assure efficient killing of the tumor cells. This requires that the tumor cell engulf the immunotoxin so that the toxin is internalized, resulting in cell death. Toxins that are currently being investigated are ricin A-chain (toxic portion) and *Pseudomonas* toxin. Unfortunately, this process would kill all nearby cells, not just the tumor cells. Another option is the attachment of a chemotherapeutic drug to the MAb. This option would in-

crease the concentration of the drug at the tumor, making it a more effective method of chemotherapy drug delivery.¹ (See Figure 3)

3.3 MAb conjugated to radionuclide

Monoclonal antibodies can also be attached to radioactive molecules/elements to deliver radiation treatment to tumor cells. The high dosage of radioactivity increases the likelihood that all of the cancer cells would be destroyed, but will kill the surrounding cells along with the tumor cells. 81C6 has previously been bound to Iodine-131, which has a half life of 8 hours. This treatment was delivered by Cokgor, et al. by directly inserting it into the tumor cavity following surgical removal of the tumor.³ This treatment limits the patients that could possibly be treated because a number of patients are not candidates for tumor removal, which makes them ineligible for this treatment. Because the residence time of 81C6 in the non-cancerous areas of the body is 36 hours, if it were administered to all patients via injection, the patient runs the risk of having other tissues destroyed by radioactivity. Also, with the radioactive iodine treatment, the patient must be quarantined during treatment because of the radioactivity of the iodine. This makes the treatment unattractive to terminally ill patients who want to spend their remaining time with family and friends.

4. Proposed Alternative Treatment Methods

4.1 Immunomicelles

A micelle is a globular structure made of a lipid tail and a polar head group, with the head groups in contact with the environment and the tails clustered in the center of the structure. According to Dr. Jeremy Berg and colleagues in the book Biochemistry, the sphere is formed to reduce hydrophobic interactions in the non-polar hydrocarbon tail.⁸ The 81C6 MAb will be attached to the polar head group of the micelle for cancer treatment. The chemotherapy drug will be located inside the micelle and will be delivered when the glioma cell engulfs the micelle. If the MAb is normally transported across the blood brain barrier, it will act as a vector for the immunomicelle.

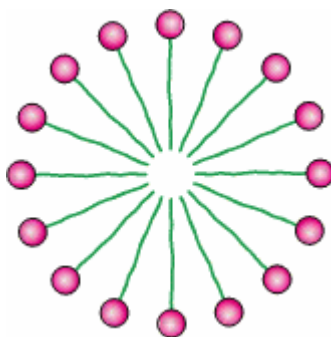


Figure 5: Cross-sectional View of a Micelle

Berg, Jeremy, et al. Biochemistry. W.H. Freeman and Co. 2002.

Immunomicelles have already been tested by Torchilin, et al. using Taxol to treat Lewis Lung Carcinoma. The cancer cell engulfed the micelle, which delivered the toxin. The micelle that was investigated was made of polyethylene glycol (PEG) – phosphatidylethanolamine conjugates. pNP-PEG-DOPE, an amphiphilic derivative of PEG, was used to attach the MAbs. Primary amino groups are attached to the pNP portion of the molecule when exposed to water. The bonds are stable urethane bonds and are readily formed at a pH of 8.0. The remaining pNP groups are spontaneously removed by

hydrolysis. The PEG derivative readily incorporates into the micelle because of the hydrophobic PEG tail. This method also allows for several MABs to be attached to the micelle.⁹

4.2 Vector Mediated Transcytosis

The major concern with the immunomicelle treatment for gliomas is that it is not known if the 81C6 immunomicelle will cross the blood brain barrier. As previously stated, a vector is a protein or antibody that has a normal predisposition to cross the BBB. OX26 is a MAB that has already been shown by Dr. U. Bickel and colleagues at UCLA to be an effective vector in aiding transport molecules across the blood brain barrier. Vectors aid in transportation across the blood brain barrier by transcytosis, which is the process of transportation across an endothelium cell by uptake and release of the cell by coated vesicles (Figure 6). OX26 undergoes receptor-mediated transcytosis by targeting transferrin. The transferrin receptor is highly expressed on brain capillary endothelial cells.²⁹ If 81C6 alone proves to not cross the blood brain barrier, a vector will then be added and tested during pre-FDA testing. The vector will be added using the same method used to attach the 81C6 MAB to the micelle.

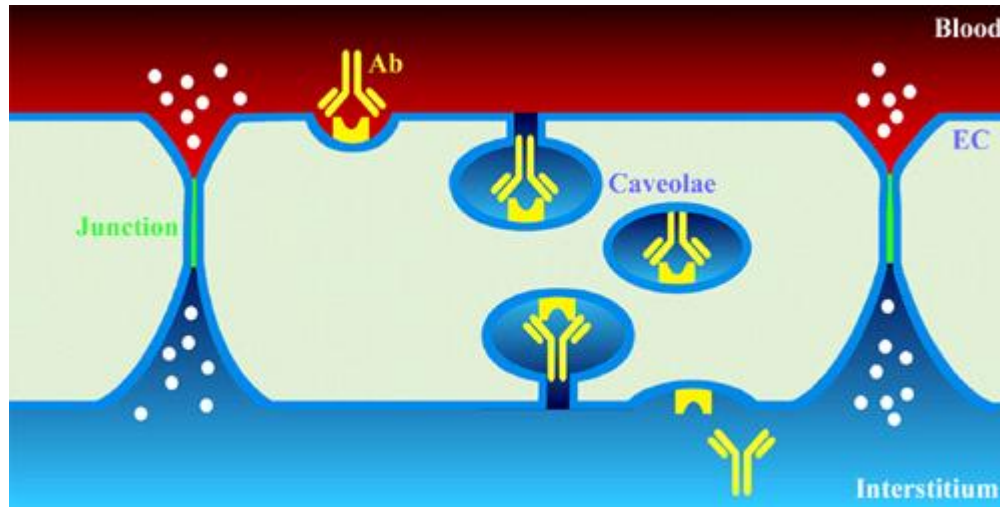


Figure 6: Vector Mediated Transcytosis

<http://images.google.com/imges>

Diffusion and accumulation of the immunomicelle inside the tumor depend on the cutoff size of the tumor blood vessel arrangement; cutoff size is a property dependant on the diameter of capillaries in the tumor. This cutoff size determines the maximum particle diameter that may be moved through the tumor. This cutoff size varies for different cancers. Torchilin et al. showed that the attachment of a MAb did not significantly affect the size of the immunomicelle; it was still small enough to be below the smallest cutoff sizes.⁹ Because the vector that will be used is also a MAb, the addition of a vector will not significantly affect the size of the immunomicelles, and will therefore not hinder uptake.

To determine the feasibility of the micelle treatment delivery method prior to beginning the FDA approval process, experiments must be conducted to determine percent micelle uptake by tumor cells both *in vitro* and *in vivo*. The micelle must also be tested for blood-brain barrier crossing to determine if a vector is necessary. The micelle must then

be tested in animals to evaluate potential side effects on the rest of body and effective tumor reduction.

4.3 Immunoliposome

Huwyler et al. have already used immunoliposomes to treat brain tumors in rats. Liposomes are comprised of subunits with a polar head group and a lipid tail, like a micelle, but the subunit is arranged in a lipid bilayer, exposing the polar head group interior and exterior of the liposome (Figure 7). In Huwyler's study an antineoplastic agent, daunomycin, was contained inside of the liposome for delivery to the tumor. This study showed that the liposome alone did not cross the blood brain barrier, but with the addition of the vector OX26 the liposome crossing of the BBB was achieved.³⁰

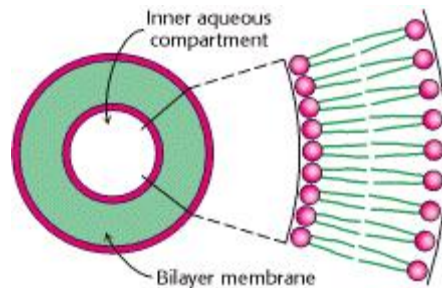


Figure 7: Cross-sectional View of a Liposome
Berg, Jeremy, et al. Biochemistry. New York. W.H. Freeman and Co.: 2002

4.4 Immunoliposomes vs. Immunomicelles

Superficially, the immunomicelle is identical to the immunoliposome. Therefore, the immunomicelle should exhibit BBB crossing. The immunomicelle exhibits superior behavior to the immunoliposome for the following reasons:

- Immunomicelles can contain more toxin than an immunoliposome of the same diameter because the immunoliposome has a thicker outer wall. This may be an advantage if the volume of the drug delivered to the patient needs to be minimized so that the treatment can be delivered via single injection instead of an I.V.
- A particle with a smaller diameter will cross the BBB more easily because less energy is required to encapsulate the particle during transcytosis.
- A very large particle may block or occupy multiple transferrin binding sites. This steric interaction may result in fewer particles to crossing the BBB.

4.5 Nanoparticles

A nanoparticle is a synthetic microscopic particle with a diameter that is measured in nanometers. Nanoparticles are used for numerous applications, including counteracting the toxicity of chemical and biological weapons, water filtration, and air purification.¹¹ However, one of the most promising applications involves a novel system of drug delivery. Laboratory investigations *in vivo* in mice by R. Reszka et. al. have shown that nanoparticles can effectively deliver cancer treatment toxins to various areas of the body, including the breasts, the lungs, and the brain.¹² Dr. Peter Ramage and colleagues have constructed nanoparticles from polybutylcyanoacrylate (PBCA), and coated with a polymer such as polysorbate 80 to enable passage through the blood-brain barrier.¹³ The image below is an electron micrograph of nanoparticles used to deliver drugs to the lungs.

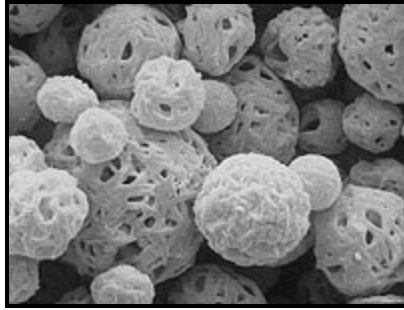


Figure 8: Electron Micrograph of Nanoparticles

Image courtesy of <http://www.betterhumans.com/News/news.aspx?articleID=2003-09-30-5>

There have been limited studies by Dr. ZR Zhang and colleagues of the use of nanoparticle-antibody conjugate systems to ensure more selective toxin delivery to breast cancer cells with fairly promising results.¹⁴ This project investigated the possibility of a nanoparticle-81C6 antibody conjugate system to selectively deliver gliomas chemotherapy drugs to gliomas brain tumor cells. Investigations revealed that this could be an effective treatment. However, there are a number of problems that must be addressed during drug delivery research which could make this option infeasible to develop at a reasonable cost. Among these problems are determining the amount of time required to release the toxin from the nanoparticle and attaching the antibody to the nanoparticle. Due to these constraints, the micelle was selected over the nanoparticle as the superior treatment delivery option. Details of the nanoparticle treatment option analysis and problems with this option are discussed in Appendix 1.

4.6 Chemotherapy Toxin Choices

Taxol[®], Temodar[®], Cisplatin, and Lomustine are a few chemotherapy agents that are currently being used to treat malignant gliomas.¹⁵ Temodar[®] was the toxin of choice for encapsulation in the immunomicelle based on its relative size. It is the smallest chemotherapy agent in terms of molecular diameter; therefore, more could be encapsulated in the

immunomicelle. Therefore fewer immunomicelles will be needed and the total volume of the treatment will be lower. This will decrease the dosage volume required, thereby reducing the likelihood that an IV will be needed in order to administer treatment. The mechanisms of the drugs are different, but they all kill rapidly dividing cells, so the side effects are similar. The dosage limiting factor for all of the drugs researched is the effects on the bone marrow and blood. Therefore, side effects are not considered in the selection of a chemotherapy toxin because each of the drugs exhibited the similar side effects.

4.7 Temodar Product Information

Dosage of Temodar[®] is determined based on the patient's body surface area (BSA) and is done in 28 day cycles. The patient receives Temodar[®] for the first 5 days then receives no drugs for 23 days. A complete blood count is done on day 22 and day 29 (day 1 of the next cycle) to determine if/when the chemotherapy should be continued. The first cycle is done at 150 mg/m² and the following cycles are done at 200 mg/m². If the absolute neutrophil count (ANC) is below 1000/ μ L or the platelet count is below 50,000/ μ L any-time during the treatment cycle then the next cycle should be reduced by 50 mg/m². The optimum duration of treatment time for Temodar[®] is not known, but the maximum treatment time during clinical trial was 2 years; this is mostly due to the truncated life span of the patient with gliomas. The short life span also results in an inability to monitor long term side effects of the drug. Temodar[®] can be continued throughout the disease progression. Dosage and treatment limiting factors were hematologic, meaning depending

on the blood. Because chemotherapy kills all rapidly growing cells, blood cells are also killed and the amount killed must be limited so the dosage is limited.¹⁹

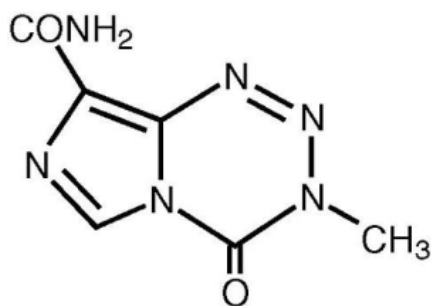


Figure 9: Temodar[®] Molecular Structure
http://www.drugs.com/PDR/Temodar_Capsules.html

5. Production of Monoclonal Antibodies

5.1 Laboratory Scale Production/Isolation of Monoclonal Antibodies

To obtain a monoclonal antibody, mice are injected with the antigen of interest. Three days following the immunization the spleen cells are extracted to obtain cells producing elevated amounts of antibodies with antigen specificity. The spleen cells are then fused with myeloma cells, or immortal lymphocytes, using PEG (polyethylene glycol). At low concentrations PEG disrupts the cell membrane enough so that cells are able to fuse together. This is done to obtain cells that will continuously produce the antibody of interest. The cells are then grown on HAT medium to select for fused cells. HAT medium contains hypoxanthine (a purine), aminopterin, and thymidine. Only cells that are fused, or hybridomas, will grow on HAT medium. Finally, the cells are screened for antibody production, so that only the antibody binding to the epitope in question is isolated (Figure 6).¹

When using murine (mouse) antibodies in treatment for humans, the human body may recognize these mouse antibodies as being foreign, an allergic response of the immune system referred to as immunogenicity. This can cause failure of the treatment due to the body's mounting of an immune response to the perceived invasion. Therefore, the MAbs must be engineered to reduced immunogenicity in humans. This can be achieved by grafting the antigen binding loop of the wanted murine MAb to the framework of a human antibody. In doing this, the antibody will still have the same antigen/antibody bonding specificity, but the human body will no longer recognize them as being foreign.¹

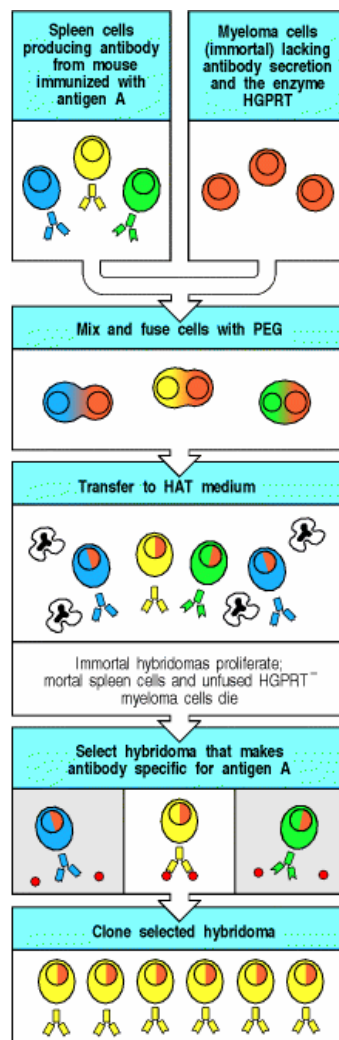


Figure 10: MAb Isolation Technique

Janeway, Charles A., et al. *Immunobiology*. 5th ed. New York: Garland Publishing, 2001.

5.2 Large Scale Production of MAbs

There are currently several approved monoclonal antibody therapeutics on the market. According to Dr. Roger G. Harrison et. al., the production of these antibodies involves three distinct production phases: a bioreaction section, a recovery section, and a purification section. The bioreaction section involves dissolving the serum-free, low protein content media powder in a water-for-injection (WFI) stainless steel tank. This involves the use of very pure water as a solvent to ensure that the media is not contaminated before exposure to the antibody. The solution is then sterilized using a dead-end polishing filter. This purified media is then transferred to a stirred tank bioreactor to grow the cells expressing the 81C6 antibody. The cells are grown in the reactor for around one week. The cells are then moved to the recovery section of the process, which involves the use of column chromatography to isolate the antibody. A membrane diafilter is first used to remove generated biomass and other suspended compounds in the mixture, and then a molecular weight cutoff ultrafilter is used to increase the solution concentration.¹⁶

Next, three types of column chromatography are used to further purify the protein solution. First, affinity chromatography is used to remove contaminant proteins. This type of chromatography involves the use of an affinity ligand that is specific to the antibody binding site. This ligand is attached to an inert chromatography matrix. This matrix will then bind to molecules according to their specificity to the binding site, while other components of the antibody mixture will pass through the medium unabsorbed. During the chromatography process the column is first equilibrated by passing a binding buffer through the column. The antibody mixture is then passed through the column and the

antibody binds to the ligand, while the rest of the mixture passes through the column. An elution buffer with a different pH or salt concentration is then passed through the column to disrupt antibody-ligand interactions and remove the antibody from the column in a separate fraction from contaminants. This process will take around one day and have a 95% recovery.¹⁶

The elution buffer is then exchanged with a salt buffer using a diafilter. This antibody solution is then further purified by the use of ion exchange chromatography. This involves the separation of molecules according to their charge. It increases the concentration of the antibody solution and removes charged contaminants. The column is packed with a charged particulate media called a resin and equilibrated with a salt buffer of opposite charge. This neutralizes the resin prior to loading the antibody solution on to the column. The antibody, which has a net charge opposite to the of the column resin, will then displace the charged salt ions and bind to the resin while the components with a lesser charge will elute through the column immediately. A salt buffer is then added to the column to displace the antibody and cause the antibody to come out of the column. This process will take around one day and have a 90% recovery.¹⁶

The antibody solution is then transferred to a stirred storage tank and ammonium sulfate is added to increase the ionic strength of the solution and prepare it for the final step in the recovery purification process: hydrophobic interaction chromatography (HIC). This is necessary to remove any final aqueous contaminants in the antibody solution. According to Dr. Helen Zgurskaya, the ammonium sulfate will cause the antibody to be less

soluble in water by neutralizing the protein surface charge and interfering with hydrogen bonding between the protein and the aqueous solution.¹⁷ The antibody solution is then eluted through the column and the insoluble proteins will aggregate on the resin beads. After the antibody has bound to the column resin the salt concentration of the elutant solution running down the column is reduced to remove the antibody from the column. This process will take around one day and a 95% recovery is expected.¹⁶

The final antibody solution is then concentrated in a molecular weight cutoff ultrafilter and the HIC buffer is exchanged with a salt buffer using diafiltration. Finally, glycerol is added to increase the antibody solution stability for relatively long term storage and the solution is sterilized using dead-end filtration.¹⁶

Figure 10 illustrates the process flow diagram of a large scale MAb production facility. The bioreaction section has the longest residence time, and is consequently the rate limiting section of the production facility. Therefore, to increase plant capacity, a second bioreaction section may be purchased and operated in sequence with the recovery and purification sections. This becomes increasingly important with the addition of a vector to the immunomicelle to ensure blood-brain barrier crossing. The vector OX26 is a MAb, and may thereby be produced using the same facility, utilizing a secondary bioreaction section.

6. Immunomicelle Production and Drug Encapsulation

6.1 Production of Immunomicelle

There are a series of steps involved in immunomicelle production. First, pNP-PEG-PE must be produced. This was done by Torchilin et. al. by placing polyethylene (PE) in a 10x molar excess of PEG-(pNP)₂ in chloroform in the presence of triethylamine. Then the organic solvents are removed. Micelles can then be formed in 0.01M HCl/ 0.15M NaCl by bath sonication. PEG and pNP can be removed from the pNP-PEG-PE by chromatography using a CL-4B column. The micelles are then freeze dried, followed by an extraction using chloroform.¹⁸

Next, the toxin is added to the micelle. First, a lipid film is formed by putting the pNP-PEG-PE/ PEG-PE mixture under vacuum. Then the toxin dissolved in methanol is added to a chloroform solution of the pNP-PEG-PE/ PEG-PE. To reform the micelles, rehydrate the solution at 50°C with 5mM sodium citrate saline and vortex for 5 minutes.⁹

In the last step, the MAb is added to the micelle (for reaction information see Figure 7). The antibody attaches to the ester group on the micelle surface because the oxygen is stabilized by the benzene-NO₂ and can detach from the micelle. One milligram of protein is added for every 10mg of pNP-PEG-PE containing liposome stored in the sodium citrate solution at pH 5.1. The pH of the solution is increased to 8.5, and then incubated for two hours to attach the antibody (protein) and hydrolyze any remaining pNP groups. Purification can be achieved by gel filtration chromatography. At the laboratory scale the maximum yield obtained by Torchilin, et al, was 60%.⁹

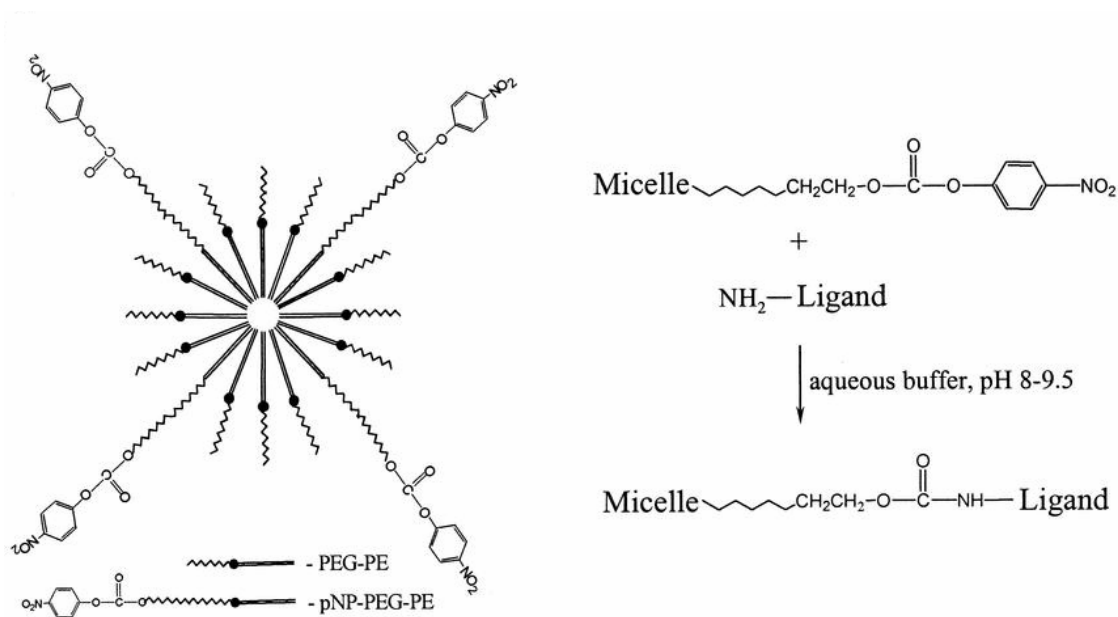


Figure 12: MAb-Micelle Attachment Reaction

6.2 Immunomicelle with Temodar[®]

In phase I of clinical trials, the first variable that should be tested is to determine the amount of immunomicelle that will deliver the same amount of Temodar[®] that is the current treatment standard. The diameter of the immunomicelle should not exceed 200nm, which was the recommended diameter for the immunomicelle treatment.⁶ The formula for the toxin is $\text{C}_6\text{H}_6\text{N}_6\text{O}_2$.¹⁹ The volume of chemotherapy drug was estimated to be 1.66×10^{-22} mL/molecule by finding the volume of each atom and then adding all of them together to get the total volume. This results in a diameter of the toxin to be 0.34 nm; a spherical assembly is assumed based on the small size and spherical nature of the molecule as displayed in the figure below. The size of the immunomicelle and the dosage will be adjusted accordingly depending on the results of the preclinical and FDA experiments. If the total amount of drug that is to be delivered is known, the volume of immunomi-

celles to be delivered can be calculated. If the volume of immunomicelles to be delivered is large then the treatment may have to be delivered by IV instead of a single injection.

7. Treatment

7.1 Blood Supply to the Brain

The brain receives blood from the internal carotid arteries and the vertebral arteries. The common carotid artery supplied blood to the head directly from the heart. It branches in the neck to form the external and internal carotid arteries. The external carotid artery supplies blood to the external cranial tissues, while the internal carotid artery supplies blood directly to the brain. The internal carotid arteries branch to form the anterior and middle cerebral arteries. The major branches that arise from the internal carotid artery supply the anterior portion of the brain with blood. Each of these gives rise to more arteries that supply the basal ganglia, thalamus, and internal capsule with blood. The posterior part of the brain gets its blood by branching of the posterior cerebral, vertebral, and basilar arteries. This supplies the brainstem, posterior cortex, and brainstem with blood.⁵ A diagram of the main branches of the vascular network in the brain can be seen below.

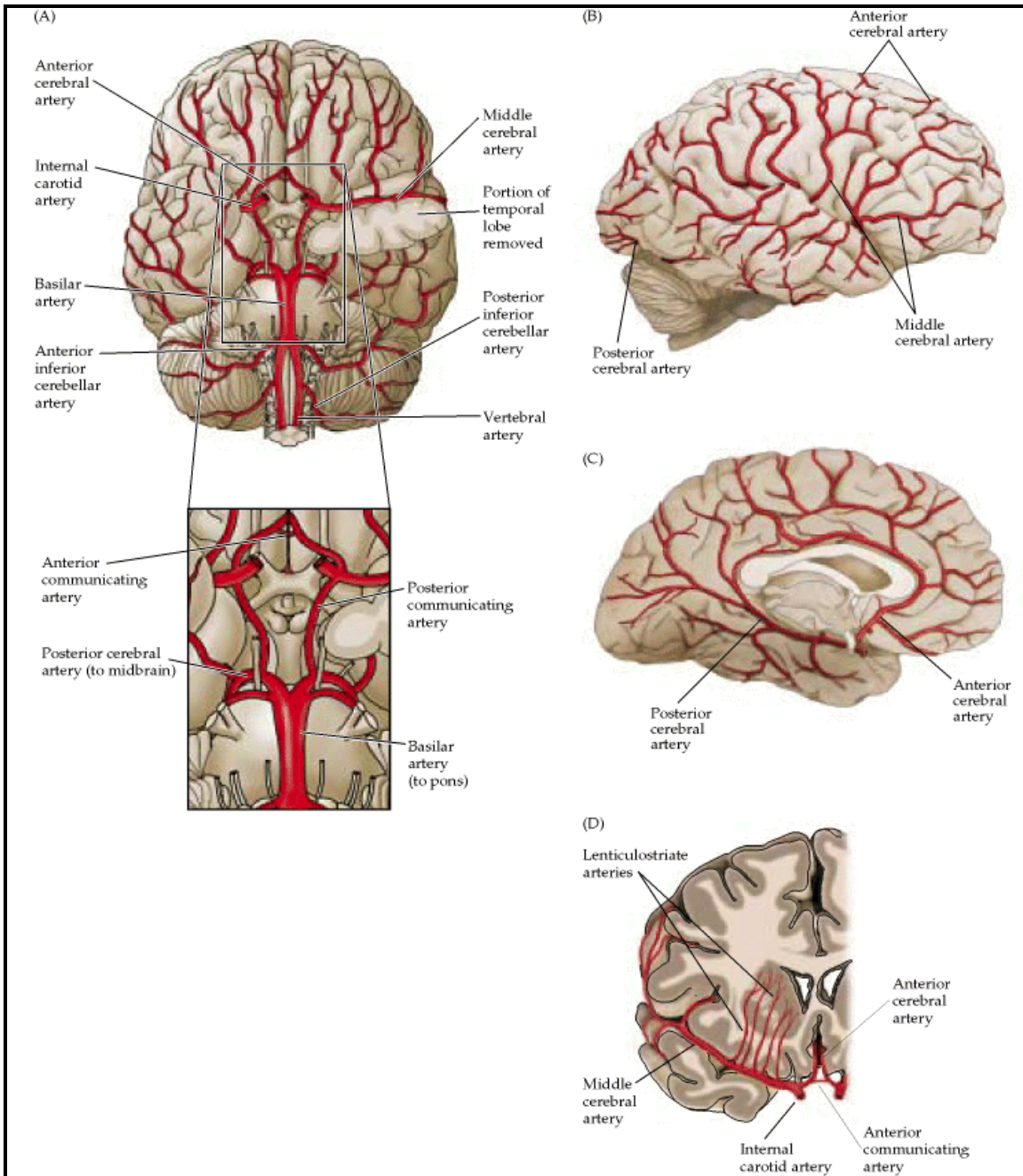


Figure 13: Vascular Network of the Brain
<http://www.ncbi.nlm.nih.gov>

7.2 Blood Temodar[®] Concentration Model

The concentration of Temodar[®] or micelles in the blood can be modeled as a function of time after treatment administration as a half-life decay process. The half life of Temodar[®] is likely greater than the half life of the micelle in the body due to Temodar[®] inter-

acting with plasma proteins in the blood. Therefore, this model will allow for comparison between the amount of time that an oral dosage of Temodar[®] remains in the body and the amount of time a micelle-contained dosage of Temodar[®] will remain in the body. The half life decay process is modeled by the differential equation

$$\frac{dC_{blood}}{dt} = -kC_{blood}$$

Separating variables and integrating with the limits $C_{blood} = C_0$ at $t = 0$ gives:

$$\ln\left(\frac{C_{blood}}{C_0}\right) = -kt$$

where C_{blood} is the concentration of Temodar[®] in the blood at time t , C_0 is the original blood concentration, and k is the half life proportionality constant. According to the Temodar[®] product information sheet, the half life of Temodar[®] in the human body is 1.8 hours; the k value can be calculated from this as 0.38 hr^{-1} using the half life decay equation.³¹ Substituting this value for k in the half life decay equation and rearranging yields:

$$\frac{C_{blood}}{C_0} = e^{-0.38t}$$

This equation models the amount of Temodar[®] in the body as a function of time with the current oral dosage treatment.

The application of this model to find the concentration of micelles in the blood as a function of time is more involved, since the half life of the micelle in the body is not known. Therefore, it must be derived by determining the rate at which micelles are removed from the body by the renal system. The typical human has around 5 liters of blood in his or her body, and the blood is pumped at 5 liters/min by the heart. Therefore, the blood is circulated through the body by the heart approximately every minute. The

kidneys receive 20-25% of the cardiac output, which is around 1 liter/min. However, they are only able to process about 13% of the blood they receive, or 120-140 mL/min. The percent of blood they would process is found as the product of the percent of cardiac output delivered to the kidneys and the percent of blood in the kidneys that is processed per minute as follows:

$$\%cleaned = \%received \times \%processed = 0.225 \times 0.13 \times 100\% = 4\% \approx 1/25$$

It is assumed that around half of the micelles in the blood cleaned are removed each time a volume of blood is processed by the kidneys. Therefore, the net percent of total blood volume for which the micelles are removed is around 2% or 1/50. Therefore, in 50 minutes the concentration of micelles in the blood is halved. From this half life a k value of 0.83hr^{-1} is calculated, which can be substituted into the half life function to create the following equation

$$\frac{C_{blood}}{C_0} = e^{-0.83t}$$

The elimination of drug from the body for an oral dosage of Temodar[®] and the elimination of drug for a micelle dosage of Temodar[®] are compared by graphing the half life function for each treatment option. The plot with these functions is displayed in Figure 12.

As clearly shown in this figure, the micelle is eliminated from the body much more rapidly than Temodar[®] alone. This phenomenon should result in a significant reduction in associated toxin side effects.

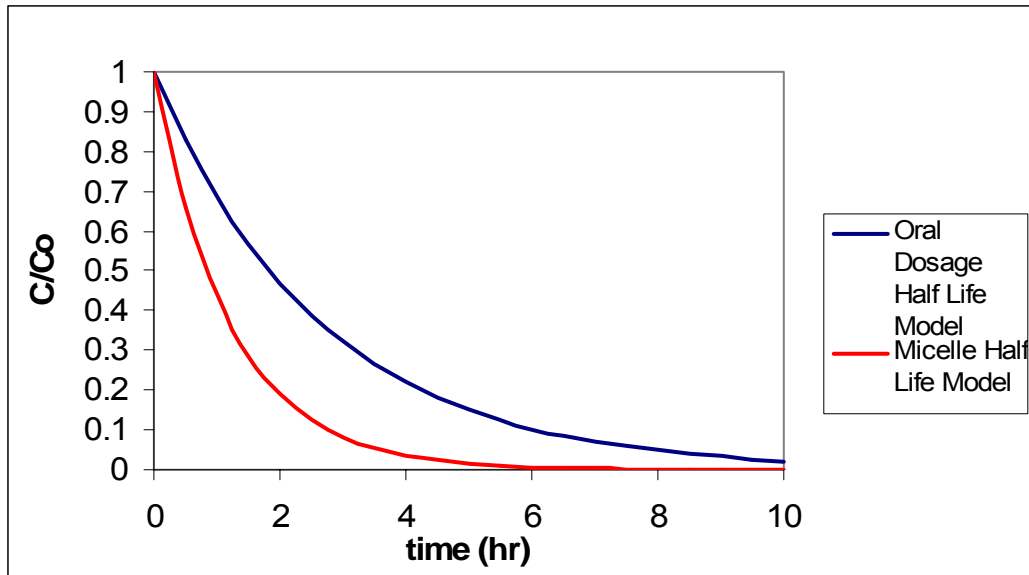


Figure 14: Micelle and Temodar® Oral Dosage Elimination Model

7.3 Drug Delivery by Injection as a Function of Tumor Volume

Rather than administering the micelle treatment orally, it is proposed to deliver the drug by direct injection into the brain in order to maximize the initial concentration of the treatment within the brain. A preliminary model for determining drug delivery to a tumor has been formulated based on drug injection methods and data concerning microvessel density within the brain tissue. It is proposed to inject the toxin containing micelle through the neck directly into the internal carotid artery (ICA). This artery branches from the common carotid artery found in the neck.³² It is necessary to inject the toxin directly into the internal artery, rather than the common artery, to avoid loss of toxin to the external branch of the carotid artery, which will result in lower concentration of toxin to the brain, as well as high concentrations of toxins in the head and face, both areas of high connective tissue content. Avoiding this arterial branch will subsequently avoid unwanted binding of 81C6 to said tissue.

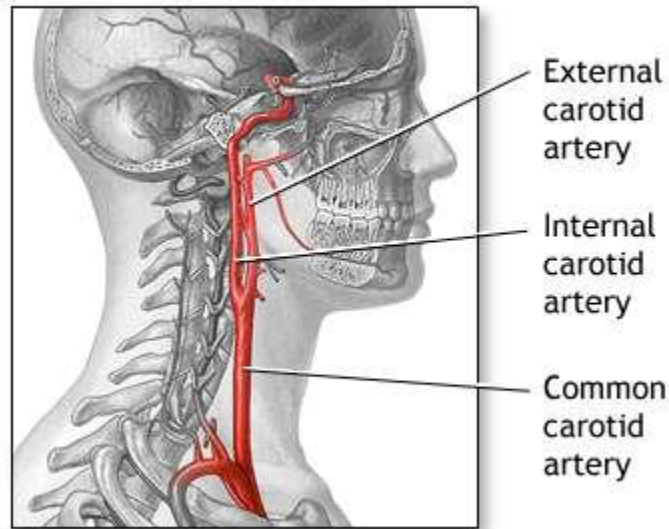


Figure 15: Common Carotid Artery Branching
www.pennhealth.com/

In constructing said model, it is assumed that only capillaries are permeable to the drug; therefore, all drug injected into the artery will remain within the vessel network until reaching the capillaries. It has been estimated that the internal carotid artery has an average flow rate of 370 mL of blood per minute.³² Assuming an injection time of five seconds, the concentration of drug entering the brain, treated as a single “plug” of high concentration, can be determined as follows:

$$\text{Dosage}/(\text{Flow rate} * \text{injection time}) = \text{initial ICA concentration}$$

Freitas³³ estimates the capillary density in the brain ranging from 2500 to 3000 capillaries per cubic millimeter of brain tissue. As tumors are invariably highly-vascularized systems, the model was constructed assuming an average tumor capillary density on the high end of this estimate, 3000 capillaries/mm³. On average, there are approximately 1400 millimeters of capillaries per mm³ of brain tissue.³² For the average brain volume of 1400 cubic centimeters, this corresponds to a total capillary length in the brain of 1.96*10⁹ mm. As the average length of a capillary is 100 μm,³² the average number of

capillaries in the brain can be estimated to be $1.96 \cdot 10^{10}$ mm. Given that each half of the brain is supplied with blood by two internal carotid arteries, for calculational purposes, this number must be halved, to represent the number of capillaries in the half of the brain supplied by the carotid artery of interest.

Using the above estimates of the microvessel network within the brain, one is able to determine the amount of drug delivered per capillary. If the branches in the blood vessels in the brain are treated as a series of splitters, with each branch resulting in the subsequent vessels containing equal drug concentration in a lower volume, one can determine the average drug contained in each capillary in the half of the brain of interest. The volume contained in each capillary is determined as follows:

$$ICA \text{ plug volume} / \text{number of capillaries} = \text{capillary plug volume}$$

The amount of drug delivered by each capillary can then be determined by the following equation:

$$\begin{aligned} & \text{Capillary plug concentration} * \text{capillary plug volume} = \\ & \text{Initial ICA plug concentration} * \text{capillary plug volume} = \text{drug delivered per capillary} \end{aligned}$$

Now, the amount of drug delivered to a tumor as a function of tumor volume is simply given as follows:

$$\begin{aligned} & \text{Drug delivered per capillary} * \text{number of capillaries per volume of tumor} = \\ & \text{drug delivered per unit tumor volume} \end{aligned}$$

A sample standard curve for this model, showing drug delivered to a tumor based on its volume, was constructed using a Temodar[®] dosage of 350 mg, based on an assumption

that 50% of the drug containing micelle will cross the BBB, and that 50% of the drug that crosses will actually bind to the tumor. This standard curve can be seen in Figure 14.

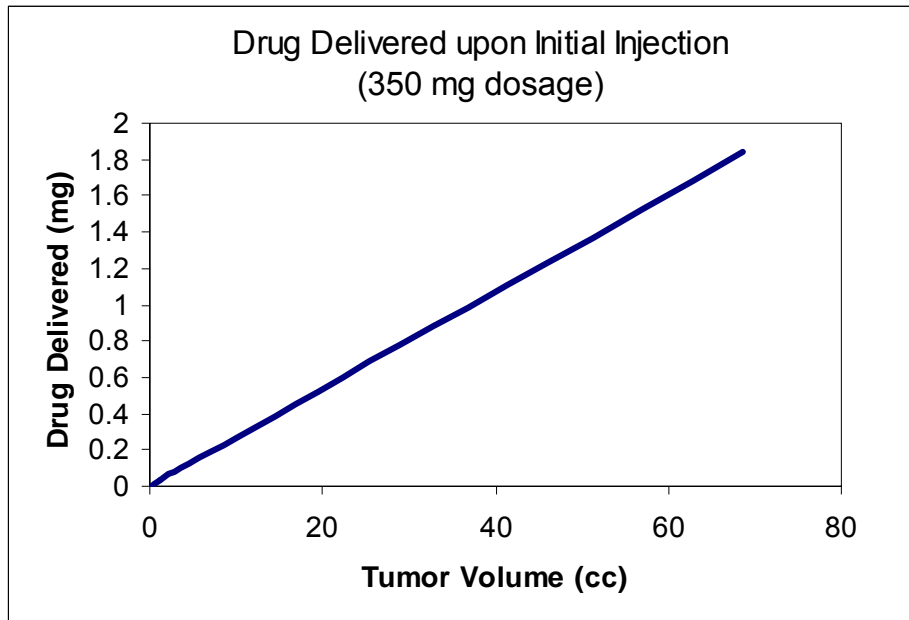


Figure 16: Drug Delivery Standard Curve

This model returns a value of $0.0268 \mu\text{g}$ drug per mm^3 tumor tissue. Applying this model to the existing method of oral dosage, assuming the 350 sample dosage is diluted in the entire 5 L of blood in the body, shows that the method of oral dosage delivers a mere $0.000107 \mu\text{g}/\text{mm}^3$ tumor, illustrating the superiority of the injection method. Injection renders a 250 fold increase in the amount of drug delivered to the tumor for an amount equal to the amount taken orally.

This preliminary model contains key assumptions. The arbitrary estimations that 50% of the drug-containing-micelle crosses the BBB and that 50% of this drug bind to the tumor have no basis in data or observation; in order to refine this model, experiments will have to be conducted during pre-FDA testing in order to determine the amount of micelle that

actually crosses the BBB and the amount of micelle that actually binds to the tumor, in order to determine the actual efficacy of the drug delivery.

7.4 Brain Immunomicelle Concentration Model

A two phase model is used to describe the changing concentration of a drug that is injected directly into an organ, in this case, the brain.³⁴ This is a standard model used in pharmacokinetics to describe the movement of injected drug through the body. In this model, the body is described by two compartments: Compartment X_1 , the organ into which the drug is injected, in this case the brain, and compartment X_2 , which represents the rest of the body. The drug is initially injected into compartment X_1 ; some of the drug will penetrate into the surrounding tissue, and the rest will be circulated throughout the body, eventually reaching concentration equilibrium.³⁵

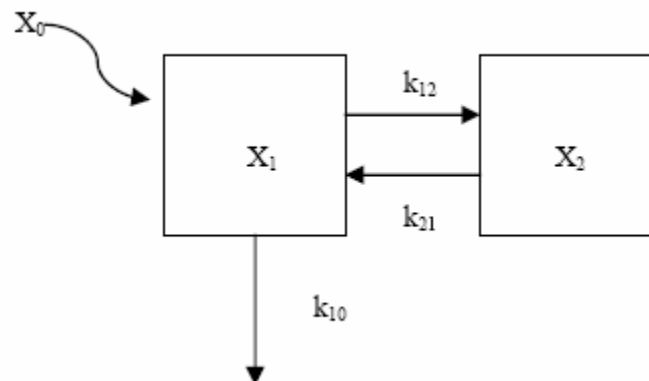


Figure 17: Two Compartment Model

The k -values are kinetic rate constants that describe the rate of movement of drug between the two compartments and into the surrounding tissues of the organ into which the drug is injected.³⁴

The change in concentration can be shown graphically by the following diagram.

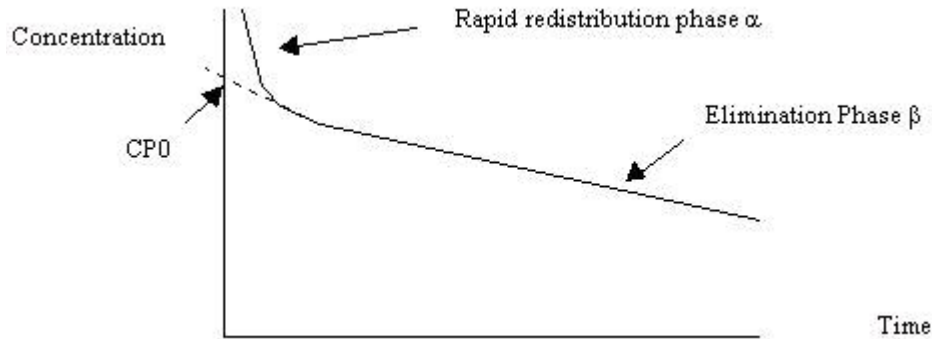


Figure 18: Equilibrium Elimination Model
www.4um.com/tutorial/science/pharmak.html

The first phase, or alpha phase, is a rapid redistribution phase that occurs after the initial injection. There is an initial high concentration of drug in the brain immediately after injection. All drug that does not penetrate into surrounding tissues during initial circulation will quickly be washed out into the rest of the body. This causes a sharp drop in drug concentration in the brain during this phase, eventually reaching equilibrium between the brain and the rest of the body. In the second phase of changing concentration shown, the beta phase, the concentration in the brain slowly and steadily decreases as the body eliminates the drug. Extrapolating this curve to zero gives the theoretical initial concentration of drug in the body if all un-absorbed drug was immediately circulated throughout the body, similar to an oral dosage, rather than directly injected.³⁴

This curve is described by the following equation, showing the bi-exponential decay of concentration with time.

$$C_{brain} = A_1e^{-\alpha T} + B_1e^{-\beta T}$$

where C_{brain} is concentration in the brain, T is time, A_1 and B_1 are intercept constants of the alpha and beta phases, respectively, and α and β are hybrid rate constants, or functions of the three rate constants presented in the two-compartment model. Additionally,

the α and β constants are also functions of the phase half-life. The β parameter was determined by assuming the half-life of the elimination phase is that calculated by the oral dosage model.

The half-life of the alpha phase was determined from the data obtained from the injection dosage model. Assuming that the brain and the body were two equally mixed vessels with blood continually circulating between them, plots of changing concentration in the brain and the body were constructed to determine the equilibrium concentration at the end of the alpha phase.

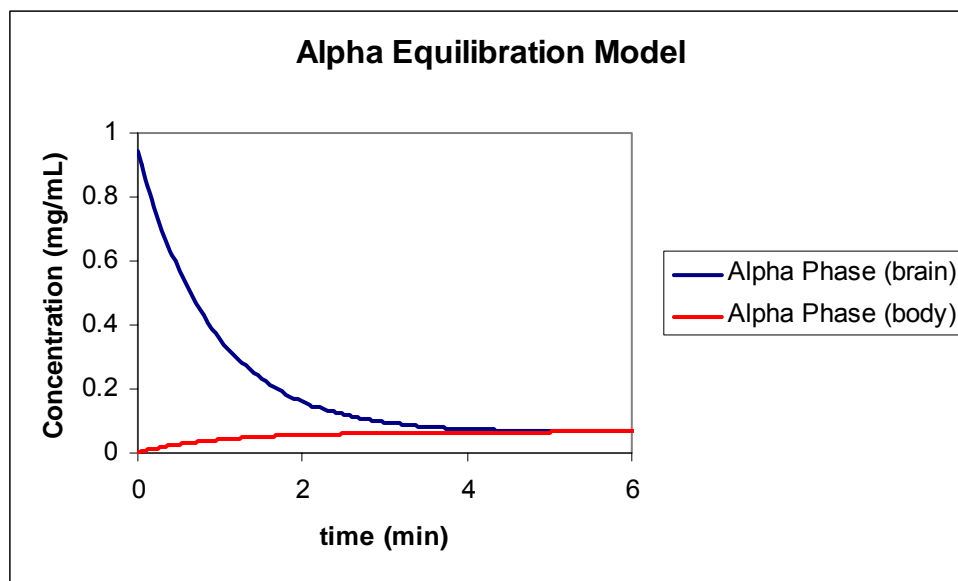


Figure 19: Redistribution Phase Equilibration Model

This model fairly accurately described the rapid redistribution of drug throughout the body, as high concentration blood left the brain and low concentration blood from the body entered the brain. From this model, the half-life of the alpha phase was calculated to be 0.0104 hr^{-1} .

The A_1 and B_1 parameters were determined from the injection model, which returned an estimate of the amount of drug exiting the brain after initial injection, or the amount of drug not absorbed by the tumor. Dividing this initial amount of drug by the amount of blood in the brain gave an estimate for A_1 , and dividing this amount of drug by the total amount of blood contained in the body gave an estimate for B_1 .

With the A_1 , B_1 , α , and β values, the relationships between the various parameters could be used to determine estimates of the kinetic rate constants in the two-compartment model based on the data from the previously presented models. The following table summarizes the results computed for a median dosage of 350 mg Temodar, assuming the 50% crossing of the BBB and 50% binding of the drug that crosses.

Table 1: Pharmacokinetic Parameters

| | |
|-------------------------------|--------|
| $t_{1/2} \alpha$ (hr) | 0.0104 |
| $t_{1/2} \beta$ (hr) | 0.8333 |
| α (hr^{-1}) | 66.54 |
| β (hr^{-1}) | 0.8318 |
| A_1 (mg/mL) | 0.9447 |
| B_1 (mg/mL) | 0.0699 |
| k_{21} (hr^{-1}) | 5.359 |
| k_{10} (hr^{-1}) | 0.8680 |
| k_{12} (hr^{-1}) | 61.15 |

These parameters, when plugged into the previously presented equation for bi-exponential decay, result in the following graph, a model of the changing concentration with time within the brain after injection, specific to the models constructed to describe the proposed procedure.

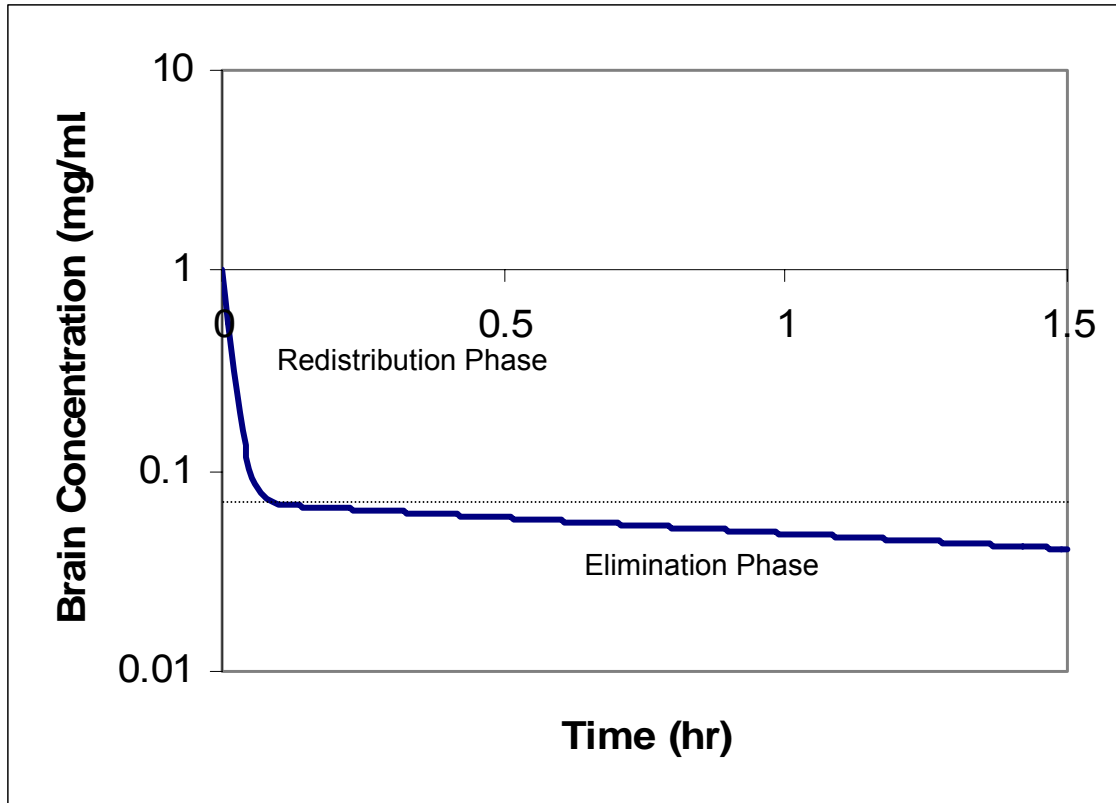


Figure 20: Micelle Two Phase Elimination Model

These parameters will be verified and/or improved upon experimental determination of assumed values used in the construction of the models from which the parameters were derived. For a more detailed description of the models used to derive these parameters, see Appendix 2. For complete model calculations, see the attached Excel[®] file “Concentration and Dosage Models.”

8. Animal Testing

There is no animal disease model for gliomas, so a mouse model must be generated in the laboratory. According to Karl Schmidt et. al., this is accomplished by obtaining nude mice and infecting them with human glioma cells, which will cause brain cancer in the mouse.²⁰ Nude mice are born without a thymus; therefore, they are unable to mount most immune responses including the killing of malignant cells, allowing for tumor formation. The nude mice can be obtained from the Jackson Laboratory for approximately \$70 per mouse.²¹ The tumor cell lines can be purchased from the American Type Culture Collection in Rockville, Missouri. Because gliomas can be either grade III or grade IV, two different cell lines must be purchased. The cell lines that are used must be tumorigenic in mice and are U87 for grade III and LN-18 for grade IV; at the American Type Culture Collection these cell lines cost \$185 and \$235, respectively.²² When determining the costs of animal testing the price for maintaining the tumor cell lines must also be considered.

9. Business Plan

9.1 Business Goals and Market Strategy

This company is dedicated to the use of monoclonal antibodies to treat the most pressing diseases affecting society. The company believes that in using cutting edge technology, such as toxin encapsulation in micelles, current treatments may be used to a more effective and less invasive measure. The goal of the company is to become a proprietary drug delivery company, using current pharmaceutical means to provide therapy for the most

demanding diseases facing society today. In this case, gliomas, or malignant brain tumors, will serve as an example of the diseases that the company hopes to treat and reduce.

In 1997, the first Monoclonal Antibody (MAb) treatment was approved for pharmaceutical use in the US by the FDA (Rituxan).²³ Today, twenty-eight antibody preparations have been approved for use in the US and Europe. Two of the approvals have since been rescinded, but 500 more are in the development stages. This represents the largest biotechnology category in development. Thus, it is important to look at the future of the MAb market, to ensure that there is not an over-saturation of the marketplace, leading to excess production and corporate losses. During 2002 and 2003, the MAb market in cancer therapy has grown at an average annual growth rate of nearly 60%.²⁴ This growth is exceptional, and represents the large interest and high effectiveness of MAb treatment of cancer. There has been nearly a \$2 billion increase in revenues for MAb treatments for cancer since 2001. More than \$3 billion in revenue was recorded for MAb for cancer treatment in 2003, with expected revenues of more than \$12 billion in 2008. The sales growth of MAb Cancer Therapies is displayed in Figure 10.²⁴ However, this explosive growth may be slowed by factors such as difficulty in obtaining HMO approvals. If the MAb treatments are not approved for use by the HMOs then the cost of the treatment will be too high for most patients. Thus, any treatment must demonstrate an increased effectiveness over current methods to be considered for approval by the HMOs. A decreased incidence of severe side effects may also be a point of consideration by the HMOs. Therefore, the selection of gliomas as a disease for treatment allows for greater success

because there are few therapies which are effective against this type of cancer, and the survival rate is quite low. Therefore, even marginal successes would be considered gains by the HMOs, leading to a higher rate of approval.

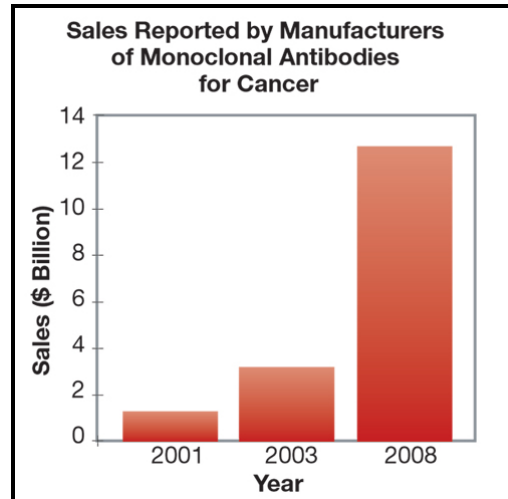


Figure 21: Sales of Monoclonal Antibodies for Cancer

Elder, Melissa. *Monoclonal Antibodies for Cancer*. Biopharm International. Volume 17, Number 11. pp 66. Advanstar Communications Publication. November 2004.

The specific rate of incidence of gliomas is two to three cases per 100,000 people per year². Therefore, using an estimate of 295 million as the population of the US, an incidence rate of six to nine thousand per year in the US may be projected.

9.2 Business Organization

Two options for the type of business have been explored, contract manufacturing and pharmaceutical manufacturing. The selection of a type of business is contingent upon the final delivery mechanism of this project. If a treatment option is selected that involves stimulating an immune response by the use of the antibody and does not require the use of a toxin, then the company should be considered a pharmaceutical company that provides treatment for cancer patients. The scope of the business will be limited to providing a safer, more effective, delivery of chemotherapy drugs to a targeted tumor without

the extensive side effects of the current chemotherapy drugs. In the business model for a drug delivery company there would be extensive resources used to promote the technology of the company to the current manufacturers of chemotherapy drugs. The ability to modify existing toxins for more controlled release would be a major selling point for the company. Expenditures would be required to develop the delivery of the specific toxin to the targeted cancer cells. This formulation and development cycle using another company's drug would be extensive and result in major costs for the company; however, in contracting with a company to provide a delivery mechanism for an existing drug, some of this cost would be deferred by the initial investment of the contracted company. This deferred cost of development and research would provide initial capital for the intensive process of adapting an existing drug to a modified delivery technique.

Another benefit of the drug delivery technology company is the ability to defer the cost of FDA approval and testing. The major steps for FDA approval for which the company is responsible are in most cases limited to the approval of the delivery technique, the facilities used for manufacturing the modified delivery system, and the materials used in said system. Another part of FDA approval, which involves the approval of the drug in connection with the delivery mechanism, would be mostly a concern of the contracted company. The FDA modeling contained in this report should serve as an estimate and a basis for a contracted company to make a decision to go forward with the incorporation of their drug into the technology provided by the company. The final payment of the full contract for development of the drug into the delivery system would be contingent upon final FDA approval, but the major capital investment needed for the FDA approval proc-

ess would not be a responsibility of the company. This business model does not require the enormous amount of capital investment required by the FDA approval of most new drugs.

In most cases the capital expended to ensure approval of a treatment can exceed several hundred million dollars. This is an enormous burden on a small and growing company. Avoiding this investment aids in the ability of the company to grow and find a stable niche in which to enter into the biotechnology and pharmaceutical industry. The long-term goal of the company would be to increase its share in the biotechnology field by becoming a company able to meld current technology with ideas of tomorrow, increasing the effectiveness of treatment while decreasing the side effects of those treatments. The ability to provide a better, safer, and more reliable treatment path will increase the viability of the company in the cancer treatment community of pharmaceuticals and biotechnology.

9.3 Glioma Incidence in the US

Two to three incidences of gliomas occur per 100,000 people in a given population per year.³ According to the US Census Bureau on January 1, 2005 the population of the United States was 295 million people.³⁶ This translates to roughly six to nine thousand cases of gliomas in the US each year. Therefore the mean number of patients suffering from gliomas per year was estimated at 7375.

The estimated population over the last 5 years, starting from the year 2005 was plotted to determine the rate of increase in the population of the US. The chart shows an increase of roughly 1% per year. This increase was used to estimate the increase in the number of incidents of gliomas in the US over the product lifetime, including all testing phases and economic production.

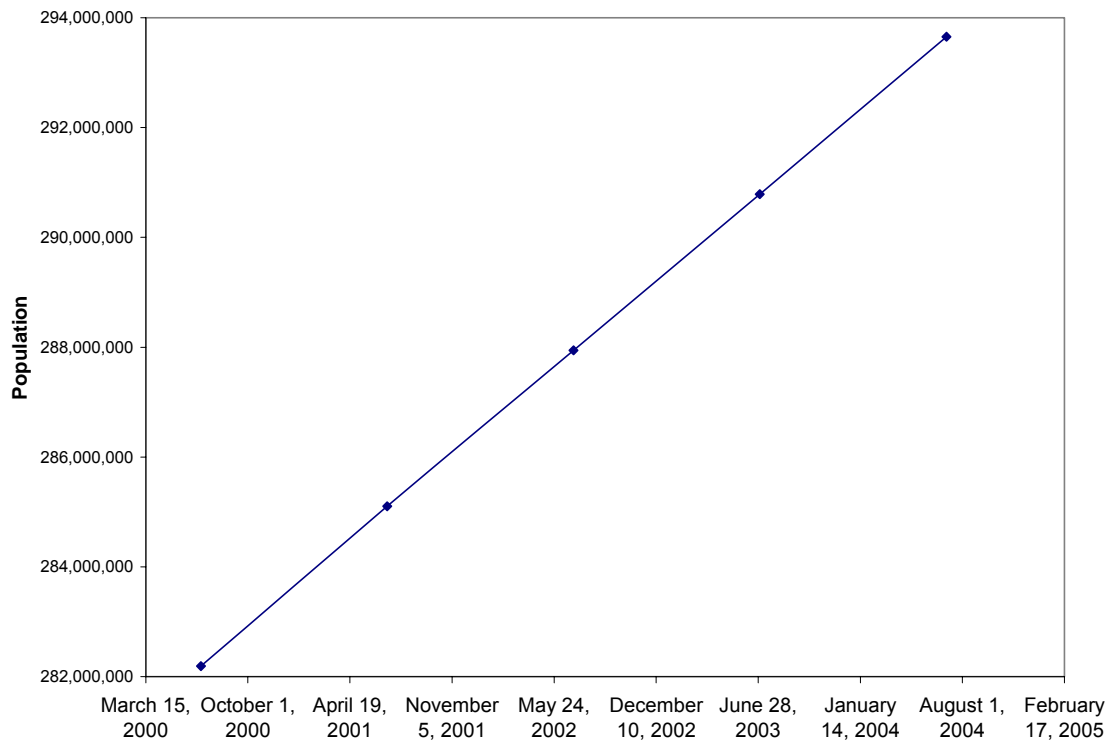


Figure 22: Population Growth of the United States

9.4 Plant Location

To determine the optimal location for the plant to produce the antibody and micelle, the first criteria given consideration was the location of the top fifty cancer research hospitals in the United States.²⁵ These were plotted on a map of the US, as shown in Figure 23. Thirty-three of the top fifty cancer research centers are located in the eastern US, east of the Mississippi River. Additionally, three of the top five hospitals are located in the

megalopolis known as the Boswash, which runs southwest from Boston to Washington DC, including Philadelphia, New York City, and Hartford, as well as all surrounding suburbs.

This 400 mile strip of land contains one of the most fertile academic environments in the world. The university medical facilities that are located in this area include Johns Hopkins Hospital, Yale Medical Facility, and Harvard Medical School. These universities offer not only a wealth of cancer research and expertise, but also vital federal funding. Many of these schools currently receive grants from institutes such as the National Institute of Health (NIH). These institutes not only rank among the top cancer treatment facilities in the nation, but also among the most well funded institutions in the US.²⁶ The average NIH grant amount at Johns Hopkins, Yale, and Harvard Universities, combined for the 2003 fiscal year, was \$450,000 dollars per grant. Combined with the universities, where much of the research and development of this new technology will be carried out, the financial gains of working with these universities is obvious. Using this criteria, it was determined that the optimal placement for a production plant and main campus for the company would be in or around New York City. This is a central location of the Boswash and gives several options for plant location. A plant could be built outside New York City in New York State, Connecticut, or New Jersey.

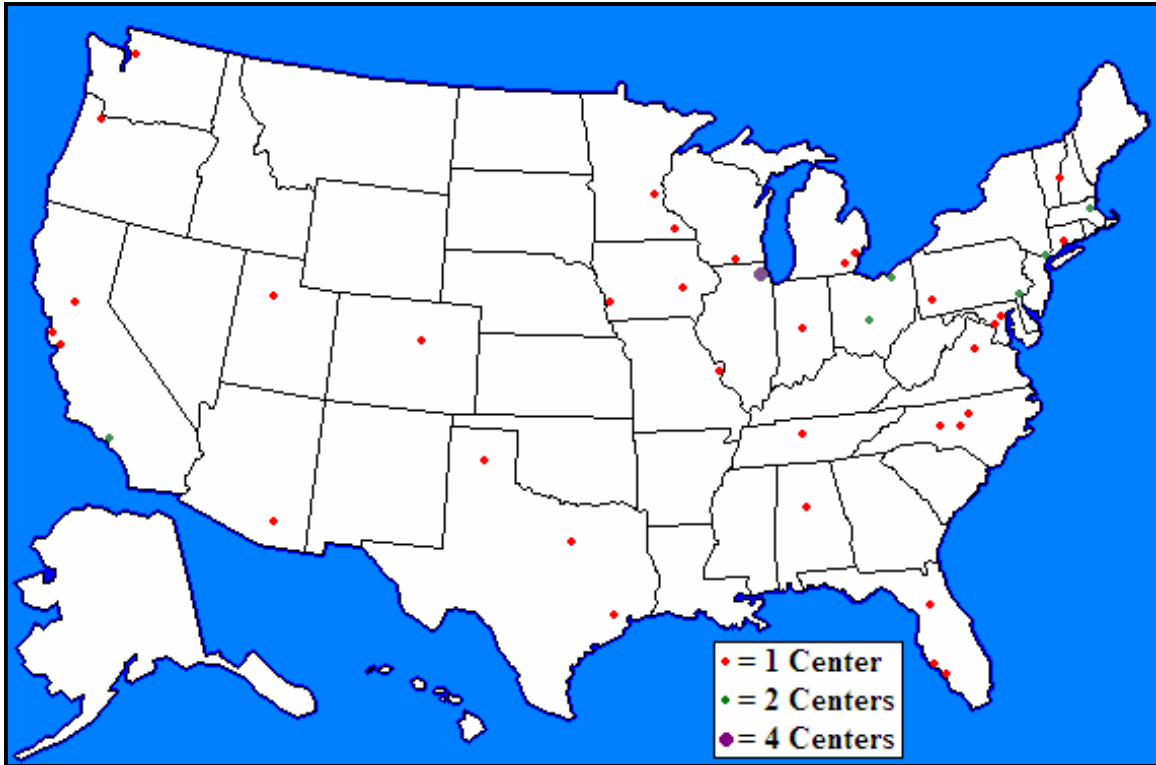


Figure 23: Location of Top 50 Cancer Treatment Centers in the US

The hospitals located in the Boswash that will be the target facilities for this treatment are:

- Memorial Sloan – Kettering Cancer Center (New York City, New York)
- Johns Hopkins Hospital (Baltimore, Maryland)
- Dana-Farber Cancer Institute (Boston, Massachusetts)
- Fox Chase Cancer Center (Philadelphia, Pennsylvania)
- Massachusetts General Hospital (Boston, Massachusetts)
- Yale – New Haven Hospital (New Haven Connecticut)
- New York Presbyterian Hospital (New York City, New York)
- Hospital of the University of Pennsylvania (Philadelphia, Pennsylvania)
- Inova Fairfax Hospital (Falls Church, Virginia)

As glioma patients frequently travel to these hospitals for treatment, a marketing strategy will initially be targeted at the oncologists at these hospitals.

9.5 Funding

On the front end of this project, the major burden for funding will be the cost of research and development for the micelle delivery mechanism. This will be funded by both private investments and government research grants. A large source of funding will be from the NIH. The major grants that will be sought from the NIH are: Small Business Technology Transfer Grants, Small Business Innovation Research Grants, Animal (Mammalian and Non-mammalian) Model and Animal and Biological Material Resource Grants, Biotechnology Resource Grant Program, and Exploratory Grants²⁷. The average values of the grants are listed in Table 2.

Table 2: Available Funding from NIH

| Grant | Average Amount per fiscal year |
|---|---------------------------------------|
| Small Business Technology Transfer (Phase I) | \$140,700 |
| Small Business Technology Transfer (Phase II) | \$318,492 |
| Small Business Innovation Research (Phase I) | \$149,261 |
| Small Business Innovation Research (Phase II) | \$425,517 |
| Animal (Mammalian and Non-mammalian) Model, and Animal and Biological Material Resource | \$716,044 |
| Biotechnology Resource Grant Program | \$1,628,377 |
| Exploratory Grants | \$1,134,298 |

Using these values for the average grants available, an estimate of the amount available per year would be \$3,768,680 for the first years of research and \$4,222,728 for subsequent years. The experiments that will be carried out with this funding are outlined in the

pre-FDA testing section of the report. These grants are all from the NIH, the major source of funding for this company.

Another source of funding for this project would be the American Cancer Society (ACS). The ACS grants money to fund research at universities; therefore, the company partnered with universities would be able to provide the salaries of several researchers and the funding for several laboratories. The maximum yearly grant from the ACS is approximately \$250,000.

These estimates do not reflect every available grant, but the ones that are easily obtained and fairly standard. The actual total funding that the company would receive would be much greater than the amount found here.

9.6 Cost

During Pre-FDA testing of the micelle, a facility will be constructed to house the research labs and testing facilities. This facility is estimated to cost \$5 million, and will house the corporate headquarters and all auxiliary systems for support of the company. This facility will remain useful even after the pre-FDA testing has been completed, serving as the headquarters for the company's research and development division.

The estimated total capital investment (TCI) for a MAb production facility is \$16.3 million. This includes all necessary construction and equipment, including bioreactors, chromatography columns, and necessary sterilization equipment. The estimated TCI for

the micelle production and attachment facility is \$45 million. This includes all necessary equipment for micelle construction, encapsulation of the toxin, and attachment of the MAb to the globular structure. If a vector is needed to assist in blood-brain barrier crossing the TCI for a facility to produce the vector is estimated at \$250,000. This is less than the facility for the MAb production, because the vector will likely be another MAb and will be operated in conjunction with existing MAb facilities.

9.7 Pre-FDA Testing

Prior to submitting for FDA, approval the drug delivery mechanism will be tested and monitored in the laboratory. Animal testing will take place in this phase. The decision tree in Figure 12 illustrates the possible pathways and outcome for the pre-FDA testing.

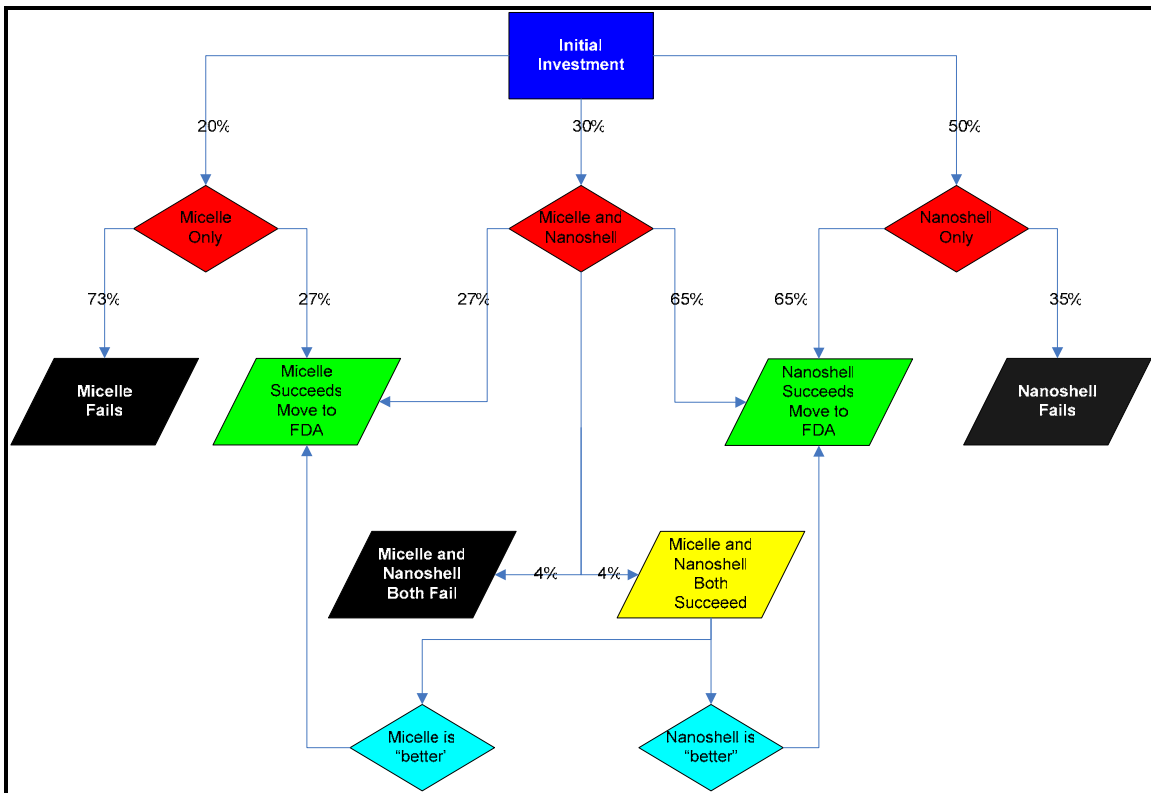


Figure 24: Pre-FDA Possibilities

Figure 25 illustrates the research and development phase of the micelle encapsulation. There are three major behaviors of the micelle and antibody that are being investigated in this section. The first aspect being investigated is cell uptake of the micelle and accompanying toxin. If the micelle delivery mechanism passes this stage and is taken up by the cell with the appropriate binding sites, then the project will progress on to BBB crossing testing. In this phase of the testing, if the MAb does not act as a vector to allow the micelle to cross the BBB, then the use of a vector attached to the micelle will be investigated. If the BBB can be crossed by the micelle then the testing will proceed to the next stage of testing. If the BBB cannot be crossed by the micelle then the project will fail.

The third stage of testing is to investigate the effects the micelle and accompanying testing will have on the rest of the body which is not cancerous. This includes all areas which have the binding site specific to the antibody as well as any areas of the body which are affected by the chemotherapy toxin. This is a comparison of the side effects of the chemotherapy alone to the micelle delivery system. If the effects on non-cancerous areas of the body are roughly equivalent to or less than the chemotherapy alone, then the final stage of Pre-FDA testing will be entered. If the effects on non-cancerous areas of the body are greater than the current chemotherapy then the project will fail.

The final stage of testing is to observe the effectiveness in reduction of the tumor. In this case it is necessary to obtain a reduction of the tumor that is at least as much as the chemotherapy alone. If there is a negligible difference in the reduction of the tumor when using the micelle as compared to the chemotherapy alone, then it becomes necessary to

evaluate the extent of the side effects. If the side effects are less than the current chemotherapy by using the micelle, then the project still has merit and should proceed. However, if the side effects are negligibly reduced then the project will fail.

Figure 26 represents a possible flow chart of the pre-FDA testing of the micelle drug encapsulation. The assigned probabilities are based on the research that has been done at each section. For some stages of testing there is no literature that specifies that the testing has been successful on some level. Therefore, the listed probabilities are simply guidelines of what might happen and are educated guesses about the process of testing. The cost listed next to each phase of testing represents the cost of materials and supplies for that phase of testing. The accompanying time that is listed with each testing phase is the time that is projected to be spent for completion of that specific phase. During pre-FDA testing the company plans to employ two PhD's and four technicians to carry out the testing procedures. The yearly salary for the PhD's is \$85,000 per year, and for the technicians the salary is at \$45,000 per year. Thus, to calculate the total cost of a specific phase of testing, it is necessary to multiply the number of employees by the annual salary of the employee giving a total labor cost per year, then multiply by the total number of years for the testing, giving the total labor cost for the specific phase of testing. The total materials cost may then be added to the labor cost for the net cost of each phase.

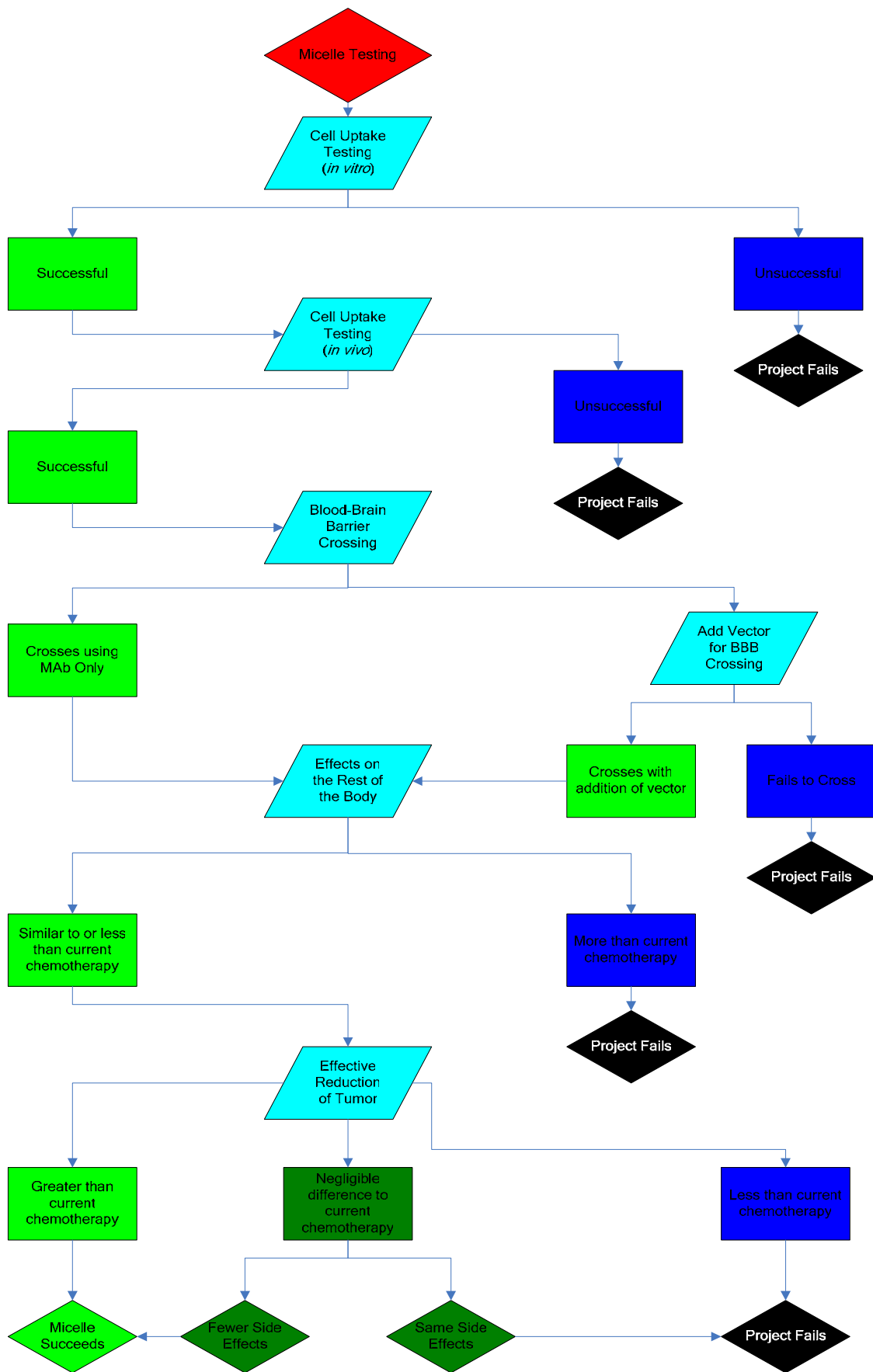


Figure 25: Pre-FDA Micelle Testing Flow Chart

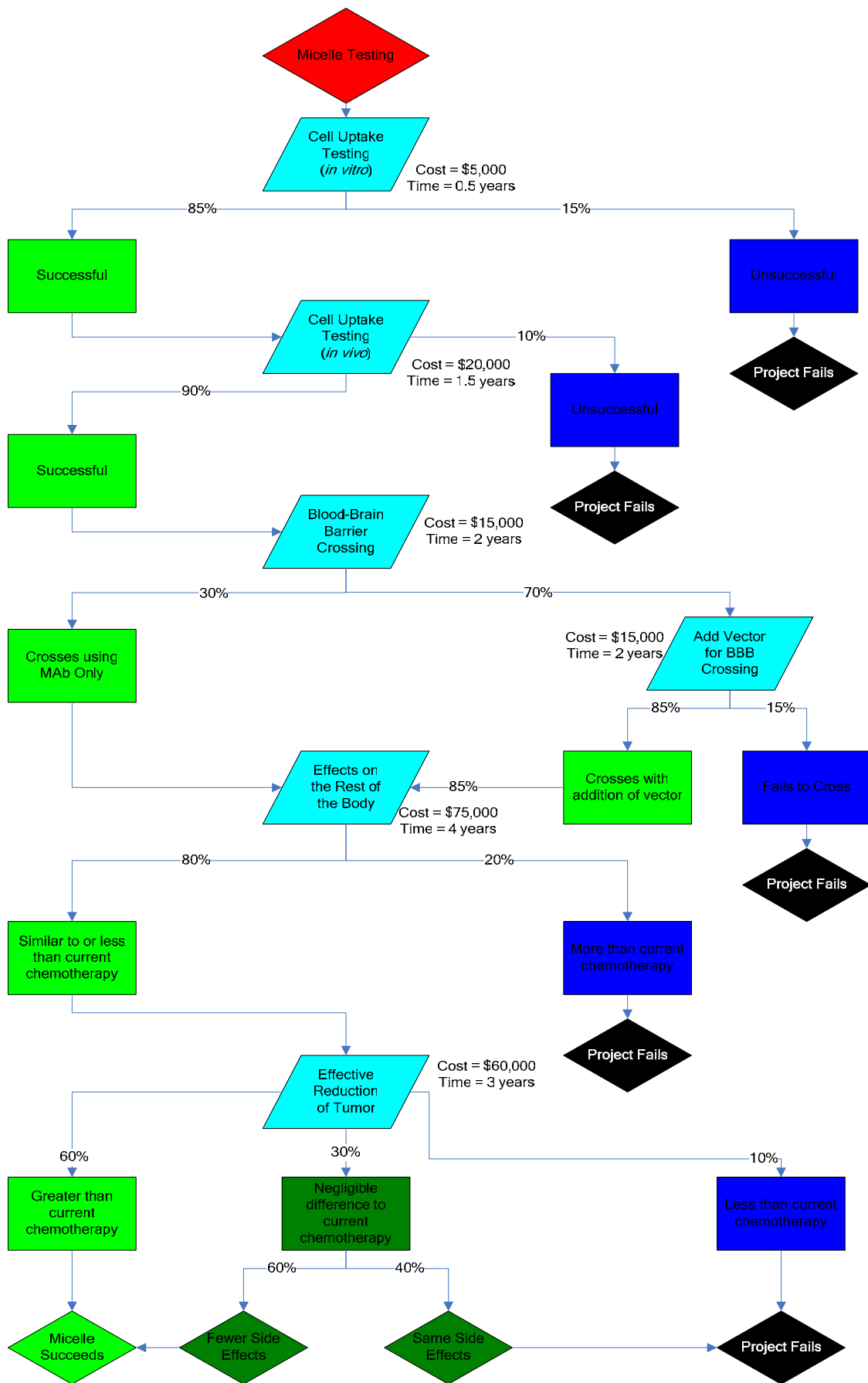


Figure 26: Pre-FDA Micelle Testing Pathways

9.8 FDA Testing and Approval

FDA testing is a long and drawn out process designed to test the effectiveness and safety of a new drug. In the case of this venture it is necessary to model the approval process of the new drug delivery technology. There are three main phases to the FDA approval process. The first phase is used to determine the dosage and immediate safety of a particular drug. The second phase is used to determine the effectiveness of the treatment and to look for immediate side effects in patient volunteers. The third phase is used to monitor effects of long term use and verify the long term effectiveness of the drugs.

For the FDA testing process, the number of doctors participating in each phase of the approval process was estimated, and the ratio of doctors to patients was kept at approximately 1:15. The amount of patients participating in each phase of the experiment was estimated conservatively based on the rate of incidence of gliomas. Therefore, the length of the phases was increased to compensate for a low participation based on the incidence of gliomas. As the testing proceeded, an increased cost in patient care was factored in for economic analysis purposes. This is due to the nature of the tests. The phase I trials monitor safety in dosage, and is therefore a very short testing period. The phase III trials monitor long term effects from long term use of the drug, therefore constituting a higher cost for patient care over the course of the treatment.

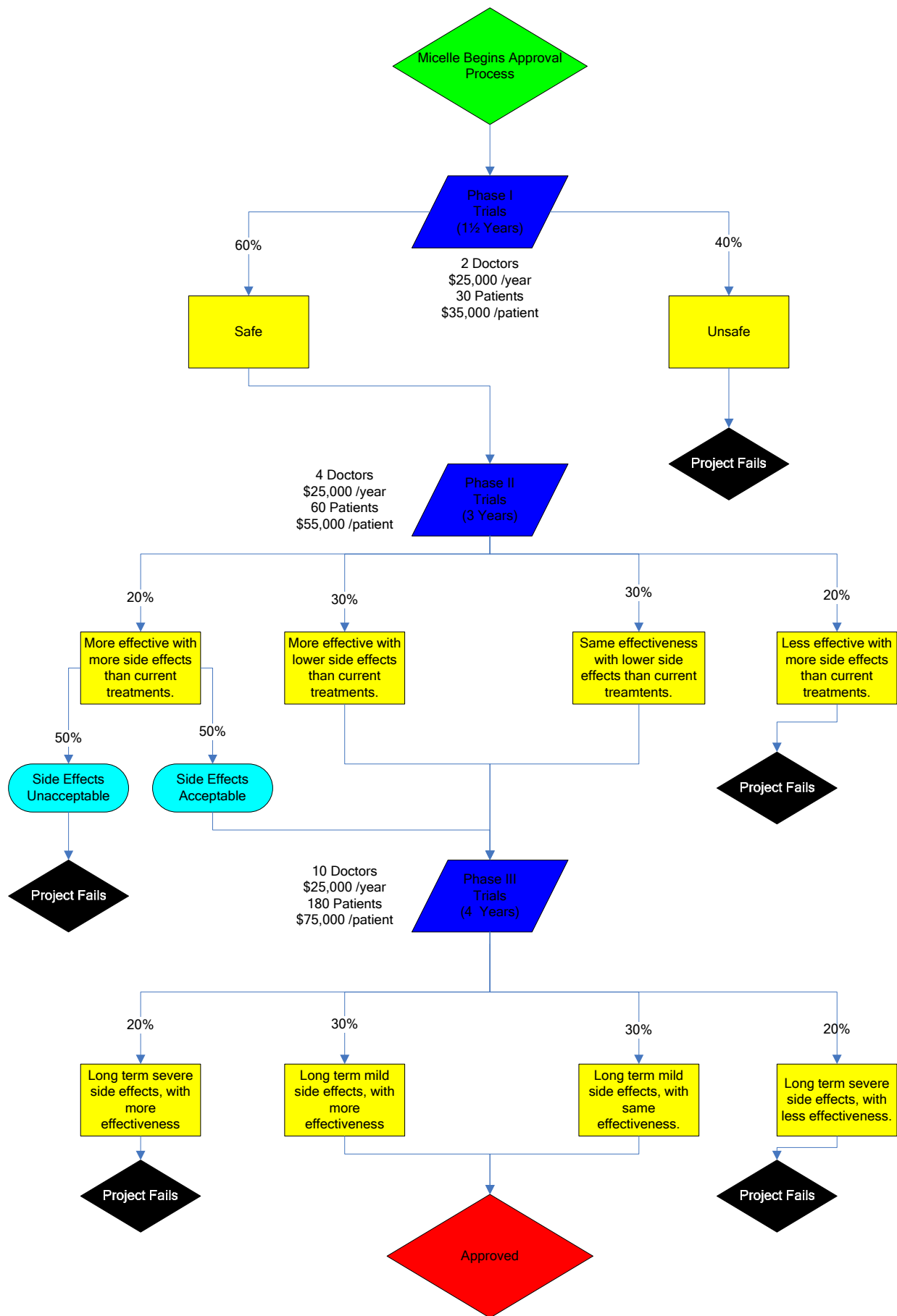


Figure 27: FDA Approval Pathways

9.9 Marketing

Once the final stages of Pre-FDA testing have begun and have shown promising results, the company will move into a phase of developing a brand name and marketing strategy. As the testing for FDA approval commences, the company will then need to retain advertising and marketing specialists. The first goal for the marketing strategy will be to target oncologists at hospitals in the New England area. This is necessary for both corporate growth and to recruit a number of oncologists for the phase two FDA trials. Marketing should not be targeted at the general public because the amount of money required to advertise to the entire nation would be quite large and this type of advertising is too indiscriminate based on the small number of glioma patients in the US.

Another facet of the marketing department's job is to bring in new business for our drug delivery technology. At the inception of the company this department will be formed. Initially, the size of the marketing department will be two people. These people will be responsible for contacting current drug manufacturers and selling the idea of monoclonal antibody targeted systems. This will generate business for the company and will provide for corporate growth.

The amount to be spent on marketing will vary depending on how rapidly the company grows and the amount of success that is observed in the pre-FDA and FDA trials. Initially, a goal of approximately \$150,000 per year will be instituted. This will provide the salary for the marketing department (2 people with salary of \$45,000 per year), travel expenses, and marketing to doctors of oncology for participation in the trials. As the trials

of our delivery technology are completed, the marketing department will need to rapidly expand. As the FDA trials progress into the phase two clinical trials the company will be looking to expand the marketing department, most likely adding two more people and additional funding for travel and marketing expenses²⁸. The budget of the marketing department will move to approximately \$450,000 per year once the FDA approval process has moved into phase III trials.

9.10 Economic Demand Model

An economic demand model was derived to account for the effects of marketing expenditures, improved treatment efficacy, and lowered treatment side effects on product demand. For a given market, two products of equal quality and prominence are described by the following the equation:

$$p_1d_1 = p_2d_2$$

In this model two treatments with an equal price would have an equal demand. However, if one product is new on the market and therefore not as well known, a knowledge multiplier α must be inserted on the other side of the equation to account for this decrease in product demand. This modified model is described by the following equation:

$$p_1d_1 = \alpha p_2d_2$$

In this derivation the α value is a fraction that is assumed to be a function of the amount of money spend on marketing during the FDA approval process and large scale production.

Since the targeted population for treatment is relatively small and concentrated in the top cancer treatment hospitals, it was assumed that once large scale production begins the demand for the treatment will grow as the oncologists become aware of the treatment and recommend it for their patients. Therefore, the rate at which the demand grows will depend upon the rate at which oncologists tell their colleagues about the new treatment and these colleagues begin recommending it to their patients. In comparison, the amount of money spent on marketing will have a negligible effect on the rate of demand growth, since oncologists are more likely to be influenced by their colleagues in the cancer treatment hospital than a visiting sales representative or magazine advertisement. Thus, the α value is assumed to be independent of the amount of money spent on marketing during phase III of the FDA approval process and large scale production.

Conversely, marketing will play an important role in the demand during the first two phases of the FDA approval process. During this period, hiring marketing consultants to promote the treatment with oncologists is critical for finding patients to participate in the clinical trials. Spending more money on marketing the product during this period of treatment development will increase the initial demand for the treatment after large scale production begins. However, these marketing expenditures will not significantly affect the long term product demand since the product demand will rapidly increase after large scale production begins as oncologists recommend the treatment for their patients.

Using these assumptions, the demand model is derived by assuming a linear increase in demand after production begins. This assumption is valid since the treatment popula-

tion is relatively small and the treatment demand will increase as the number of oncologists recommending the treatment increases. Therefore, a demand for each year can be calculated by assuming a constant annual demand increase and adding this increase to the demand of the previous year. The rate at which the annual demand changes is modeled by assuming the initial product demand is 15% of the potential product demand when the minimal annual marketing expenditures of \$150,000 are selected. The amount of time required to reach the maximum product demand is assumed as six years. The rate at which the demand increases is then calculated as

$$\frac{1 - \text{initial percent of potential demand}}{6 \text{ years}} = \frac{1 - 0.15}{6 \text{ yrs}} = 0.14 \text{ yr}^{-1}$$

Thus the final α function for the minimal annual marketing expenditure is described by the equation

$$\alpha = \text{rate of demand increase} \times \text{year} + \text{initial potential demand}$$

For the minimal potential marketing investment this equation is

$$\alpha = 0.14 \text{ yr}^{-1} (\text{year}) + 0.15$$

This model was derived by the same method for annual FDA phase I and II marketing expenditures of \$1,000,000, \$1,825,000, \$2,250,000. The plot created from these equations is shown in Figure 28.

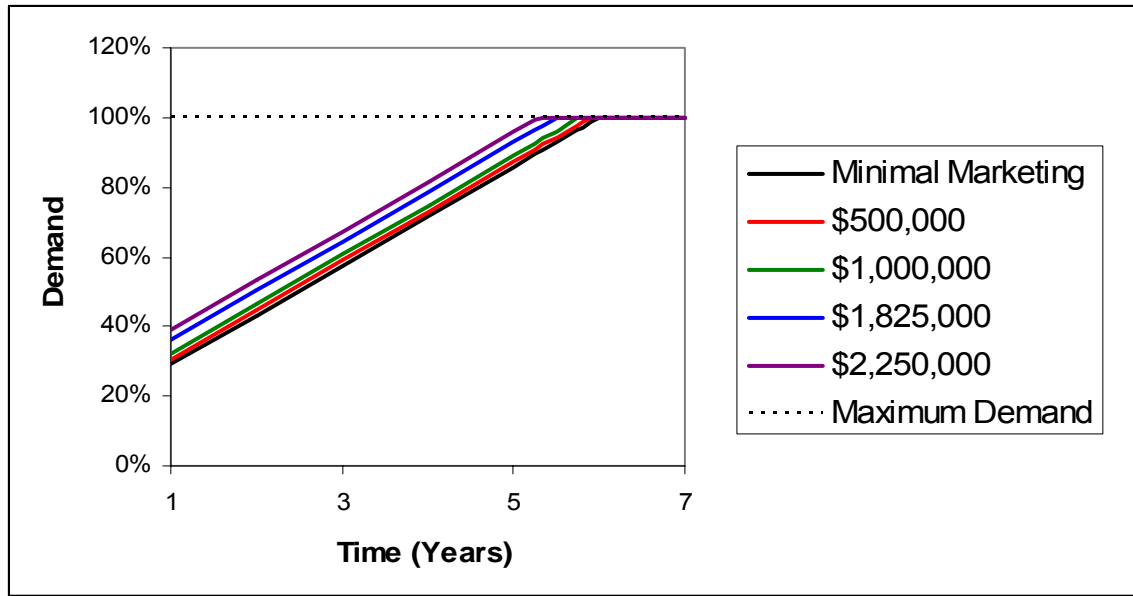


Figure 28: α Function Model

This model is completed by considering the demand increase due to improved treatment efficacy and decreased side effects. This modified model is shown in the following equation:

$$\beta p_1 d_1 = \alpha p_2 d_2$$

From this equation it can be deduced that as treatment efficacy increases or side effects decrease, the value of β will decrease as the micelle treatment demand (d_1) will increase. For each of the areas of product superiority the demand increase is modeled as 25% of the total demand (D) of 7375 patient with

$$D = d_1 + d_2 = 7375$$

Therefore, the d_1 value will be 3688 patients if the treatment is equal in quality to the current treatment, 5532 if the treatment has the less side effects or improved efficacy over the current treatment option, and 7375 if the treatment has less side effects and improved efficacy over the current treatment option.

This economic demand model is incorporated into the final profitability calculations and risk analysis. Results indicate that changing the marketing expenditures during phases I and II has minimal effects on the net present value after 15 years. However, the changes in demand based on the micelle treatment superiority over the current treatment were significant. As expected, the net present value of the project doubled when the treatment had both improved efficacy and less side effects. This indicates that treatment superiority over the current treatment has a much greater impact on product demand than marketing expenditures.

9.11 Risk Analysis

Risk analysis was performed on profitability of the micelle development and production process. The probability of each scenario of success and failure during pre-FDA and FDA testing is evaluated by multiplying the assigned probabilities of each stage of testing to determine the final probability of each success or failure scenario. For example, the probability that the micelle will not be able to be modified to cross the blood-brain barrier was found as follows:

$$P_{\text{micelle does not cross blood brain barrier}} = P_{\text{successful micelle uptake in vitro}} \times P_{\text{successful micelle uptake in vivo}} \\ \times P_{\text{vector added to cross the blood-brain barrier}} \times P_{\text{micelle does not cross blood brain barrier with vector}}$$

substituting values from the pre-FDA micelle testing flowchart:

$$P_{\text{micelle does not cross blood brain barrier}} = 0.85 * 0.90 * 0.70 * 0.15 = 0.08$$

Charts displaying the probabilities of all possible scenarios are displayed below with respect to varying investment as first-stage decisions. The accuracy of the probabilities was verified by adding all the probabilities to ensure that the sum of the pre-FDA probabilities is equal to one and that the sum of the probabilities of each set of FDA scenarios

based on each success scenario from pre-FDA testing is equal to the probability of this successful scenario occurring in pre-FDA testing.

The first stage decisions, involving amount of money spent on research and development through pre-FDA and FDA testing, were varied. Subsequent changes were made to the probabilities of successful pathways corresponding to an increased spending resulting in more likelihood of success.

Table 3: Pre-FDA Pathway Probabilities

| Pre-FDA Scenario | Probability | | | |
|---|---------------------------------|-----------------------------------|-------------------------------|---|
| | <i>Minimal R&D Spending</i> | <i>Increased pre-FDA Spending</i> | <i>Increased FDA spending</i> | <i>Increased pre-FDA and FDA spending</i> |
| No Micelle Uptake, In Vitro Testing | 15.00% | 10.00% | 15.00% | 10.00% |
| No Micelle Uptake, In Vivo Testing | 8.50% | 4.50% | 8.50% | 4.50% |
| No Blood Brain Barrier Crossing | 2.18% | 1.66% | 2.18% | 1.66% |
| Crosses with MAb, More Effects on Body | 0.19% | 0.05% | 0.19% | 0.05% |
| Crosses with Vector, More Effects on Body | 3.52% | 1.63% | 3.52% | 1.63% |
| Crosses with MAb, Less Reduction of Tumor | 0.23% | 0.25% | 0.23% | 0.25% |
| Crosses with Vector, Less Reduction of Tumor | 4.19% | 7.97% | 4.19% | 7.97% |
| Crosses with MAb, Same Reduction of Tumor, Same Side Effects | 0.07% | 0.01% | 0.07% | 0.01% |
| Crosses with Vector, Same Reduction of Tumor, Same Side Effects | 1.26% | 0.40% | 1.26% | 0.40% |
| Crosses with MAb, More Reduction of Tumor | 2.73% | 2.01% | 2.73% | 2.01% |
| Crosses with Vector, More Reduction of Tumor | 50.23% | 63.72% | 50.23% | 63.72% |
| Crosses with MAb, Same Reduction of Tumor, Less Side Effects | 0.61% | 0.24% | 0.61% | 0.24% |
| Crosses with Vector, Same Reduction of Tumor, Less Side Effects | 11.30% | 7.57% | 11.30% | 7.57% |
| Total Probability | 100.00% | 100.00% | 100.00% | 100.00% |

Table 4: FDA Approval Process Probabilities

| FDA Scenarios for Immunomicelle Crossing with MAb, Greater Reduction of Tumor | Probability | | | |
|--|---------------------------------|-----------------------------------|-------------------------------|---|
| | <i>Minimal R&D Spending</i> | <i>Increased pre-FDA Spending</i> | <i>Increased FDA spending</i> | <i>Increased pre-FDA and FDA spending</i> |
| Phase I, Product Unsafe | 0.27% | 0.20% | 0.14% | 0.10% |
| Phase II, Less Effective with More Side Effects | 0.25% | 0.18% | 0.13% | 0.10% |
| Phase II, More Effective with More Unacceptable Side Effects | 0.09% | 0.06% | 0.04% | 0.03% |
| Phase III, ST: More Effective, Acceptable SEs, LT: Less Effective, Severe SEs | 0.02% | 0.02% | 0.01% | 0.01% |
| Phase III, ST: More/Same Effective, Less SEs, LT: Less Effective, Severe SEs | 0.29% | 0.22% | 0.23% | 0.17% |
| Phase III, ST: More Effective, Acceptable SEs, LT: More Effective, Severe SEs | 0.02% | 0.02% | 0.01% | 0.01% |
| Phase III, ST: More/Same Effective, Less SEs, LT: More Effective, Severe SEs | 0.29% | 0.22% | 0.23% | 0.17% |
| Phase III, ST: More Effective, Acceptable SEs, LT: More/Same Effective, Mild SEs | 0.11% | 0.08% | 0.07% | 0.05% |
| Phase III, ST: More/Same Effective, Less SEs, LT: More/Same Effective, Mild SEs | 1.37% | 1.01% | 1.86% | 1.38% |
| Total Probability | 2.73% | 2.01% | 2.73% | 2.01% |

Table 5: FDA Approval Process Probabilities

| <i>FDA Scenarios for Immunomicelle Crossing with Vector, Greater Reduction of Tumor</i> | Probability | | | |
|--|---------------------------------|-----------------------------------|-------------------------------|---|
| | <i>Minimal R&D Spending</i> | <i>Increased pre-FDA Spending</i> | <i>Increased FDA spending</i> | <i>Increased pre-FDA and FDA spending</i> |
| Phase I, Product Unsafe | 5.02% | 6.37% | 2.51% | 3.19% |
| Phase II, Less Effective with More Side Effects | 4.52% | 5.73% | 2.39% | 3.03% |
| Phase II, More Effective with More Unacceptable Side Effects | 1.58% | 2.01% | 0.72% | 0.91% |
| Phase III, ST: More Effective, Acceptable SEs, LT: Less Effective, Severe SEs | 0.44% | 0.56% | 0.17% | 0.21% |
| Phase III, ST: More/Same Effective, Less SEs, LT: Less Effective, Severe SEs | 5.42% | 6.88% | 4.29% | 5.45% |
| Phase III, ST: More Effective, Acceptable SEs, LT: More Effective, Severe SEs | 0.44% | 0.56% | 0.17% | 0.21% |
| Phase III, ST: More/Same Effective, Less SEs, LT: More Effective, Severe SEs | 5.42% | 6.88% | 4.29% | 5.45% |
| Phase III, ST: More Effective, Acceptable SEs, LT: More/Same Effective, Mild SEs | 2.06% | 2.61% | 1.34% | 1.69% |
| Phase III, ST: More/Same Effective, Less SEs, LT: More/Same Effective, Mild SEs | 25.31% | 32.12% | 34.36% | 43.58% |
| Total Probability | 50.23% | 63.72% | 50.23% | 63.72% |

Table 6: FDA Approval Process Probabilities

| FDA Scenarios for Immunomicelle Crossing with MAb, Same Reduction of Tumor | Probability | | | |
|---|---------------------------------|-----------------------------------|-------------------------------|---|
| | <i>Minimal R&D Spending</i> | <i>Increased pre-FDA Spending</i> | <i>Increased FDA spending</i> | <i>Increased pre-FDA and FDA spending</i> |
| Phase I, Product Unsafe | 0.06% | 0.02% | 0.03% | 0.01% |
| Phase II, Less Effective with More Side Effects | 0.06% | 0.02% | 0.03% | 0.01% |
| Phase II, More Effective with More Unacceptable Side Effects | 0.02% | 0.01% | 0.01% | 0.00% |
| Phase III, ST: More Effective, Acceptable SEs, LT: Less Effective, Severe SEs | 0.01% | 0.00% | 0.00% | 0.00% |
| Phase III, ST: More/Same Effective, Less SEs, LT: Less Effective, Severe SEs | 0.07% | 0.03% | 0.05% | 0.02% |
| Phase III, ST: More Effective, Acceptable SEs, LT: More Effective, Severe SEs | 0.01% | 0.00% | 0.00% | 0.00% |
| Phase III, ST: More/Same Effective, Less SEs, LT: More Effective, Severe SEs | 0.07% | 0.03% | 0.05% | 0.02% |
| Phase III, ST: More Effective, Acceptable SEs, LT: More/Same Effective, Mild SEs | 0.03% | 0.01% | 0.02% | 0.01% |
| Phase III, ST: More/Same Effective, Less SEs, LT: More/Same Effective, Mild SEs | 0.31% | 0.12% | 0.42% | 0.16% |
| Total Probability | 0.61% | 0.24% | 0.61% | 0.24% |

Table 7: FDA Approval Process Probabilities

| <i>FDA Scenarios for Crosses with Vector, Same Reduction of Tumor</i> | Probability | | | |
|--|---------------------------------|-----------------------------------|-------------------------------|---|
| | <i>Minimal R&D Spending</i> | <i>Increased pre-FDA Spending</i> | <i>Increased FDA spending</i> | <i>Increased pre-FDA and FDA spending</i> |
| Phase I, Product Unsafe | 1.13% | 0.76% | 0.57% | 0.38% |
| Phase II, Less Effective with More Side Effects | 1.02% | 0.68% | 0.54% | 0.36% |
| Phase II, More Effective with More Unacceptable Side Effects | 0.36% | 0.24% | 0.16% | 0.11% |
| Phase III, ST: More Effective, Acceptable SEs, LT: Less Effective, Severe SEs | 0.10% | 0.07% | 0.04% | 0.03% |
| Phase III, ST: More/Same Effective, Less SEs, LT: Less Effective, Severe SEs | 1.22% | 0.82% | 0.97% | 0.65% |
| Phase III, ST: More Effective, Acceptable SEs, LT: More Effective, Severe SEs | 0.10% | 0.07% | 0.04% | 0.03% |
| Phase III, ST: More/Same Effective, Less SEs, LT: More Effective, Severe SEs | 1.22% | 0.82% | 0.97% | 0.65% |
| Phase III, ST: More Effective, Acceptable SEs, LT: More/Same Effective, Mild SEs | 0.46% | 0.31% | 0.30% | 0.20% |
| Phase III, ST: More/Same Effective, Less SEs, LT: More/Same Effective, Mild SEs | 5.70% | 3.81% | 7.73% | 5.18% |
| Total Probability | 11.30% | 7.57% | 11.30% | 7.57% |

The low calculated probabilities of success reflect the volatile nature of the biotechnology industry. As there are many areas of biology about which little is understood, technology ideas that seem like they might be profitable often run into problems during pre-FDA research and development and the long and difficult FDA approval process. Many drugs

enter the FDA approval process and relatively few are approved for sales. Therefore, there are many more failure scenarios than success scenarios in the pre-FDA and FDA flowcharts and this business venture has very high risk.

The complete product cost for treatment was determined by calculating the treatment cost necessary to recover all investments in pre-FDA and FDA research and development testing, facilities, labor, and marketing in three years. The net present value was calculated with the following formula:

$$NPV = \sum_{i=1}^{15} \frac{price \times sales - TCI}{(1 + iR)^{t(path)}}$$

The solver function in Excel[®] was used to find the treatment price necessary to have a net present value of zero after 3 years of sales for the success scenario with the highest probability, which is the scenario that the micelle crossing the blood-brain barrier with a vector and results in a greater reduction of the tumor than the current treatment. The recovery period was set at three years in order to generate enough revenues to recover the initial investment quickly. The calculated price was equal to around \$9,000 with the three year recovery period, based on annual sales to 7375 patients modified by the appropriate demand multiplier. The patient cost of the treatment was then set to \$15,000 to ensure a profit margin to compensate for the expensive nature of this project. The expected NPV for the venture was described by the following chart, wherein the expected net present values of all possible pathways were arranged from least to greatest, and the associated probabilities of each pathway were added, forming a cumulative graph of probability vs. expected NPV shown in Figure 29.

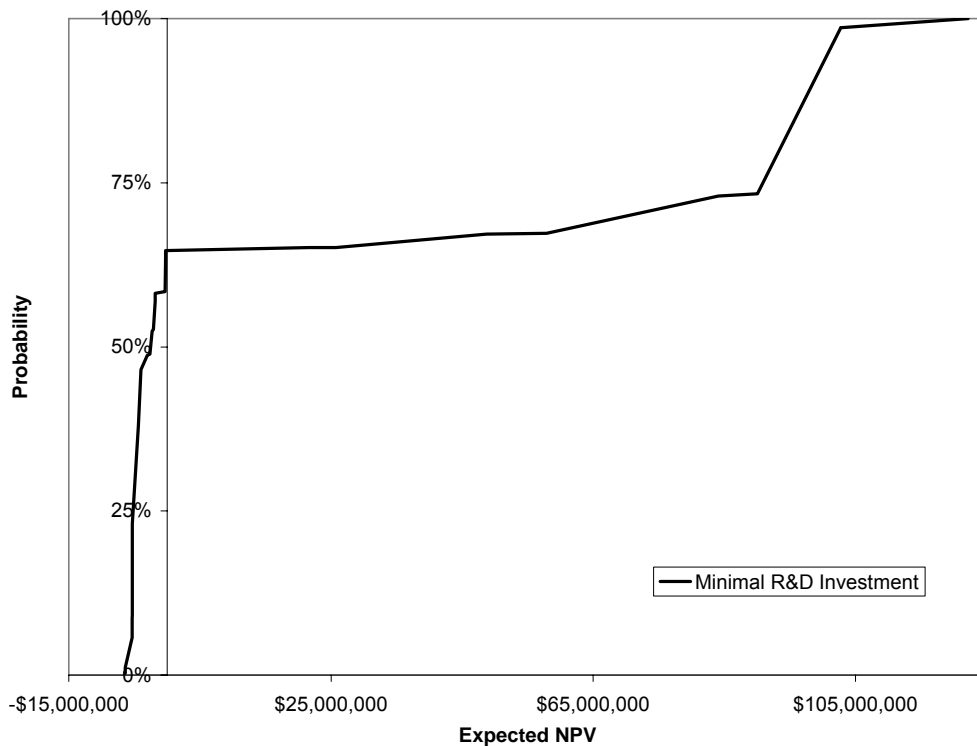


Figure 29: NPV Risk Curve for Minimal R&D Spending

Risk curves based on different first-stage decisions were then generated by varying the amount of spending in pre-FDA testing, FDA testing, and both pre-FDA and FDA testing. The maximum attainable NPV of the project decreased with the increase in spending, however more spending in the testing phases results in a higher probability of success. Figure 30 illustrates the overlay of each set of first stage decisions (minimal R&D spending, increased pre-FDA spending, increased FDA spending, and increased pre-FDA and FDA spending). Figure 30 illustrates the distribution of NPV based for each pathway that results in success, based on the minimal research and development spending. This chart illustrates the distribution of NPV based on economic factors, such as total number of sales and total facilities costs. Successful scenarios were carried out to a 15 year project lifetime. More detailed calculations can be found in the spreadsheet file attached to this report.

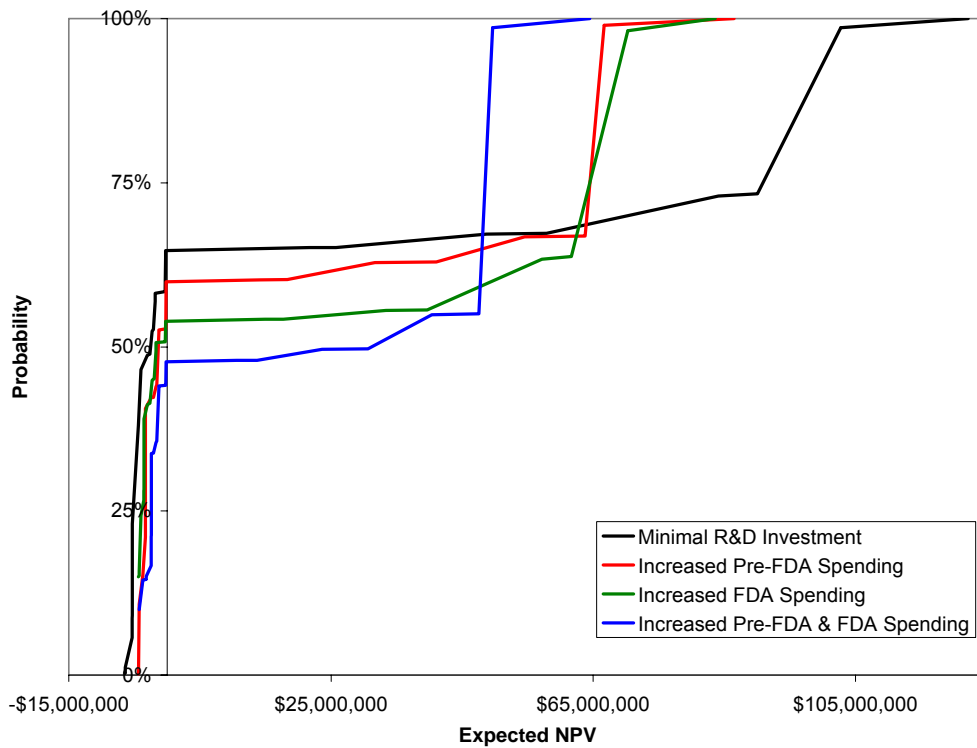


Figure 30: Risk Curves for Varying First-Stage Decisions

Figure 31 demonstrates the NPV at 5 years of the most likely success of the project. This was the scenario that was used to determine the price of the treatment and is therefore relevant as an assessment of the economic viability at 5 years following the successful completion of FDA approval. The length of time to recover the initial investment was set at three years, so at five years a profit should be clearly visible, as is shown in the chart. The chart is also shown on the basis of minimal research and development spending.

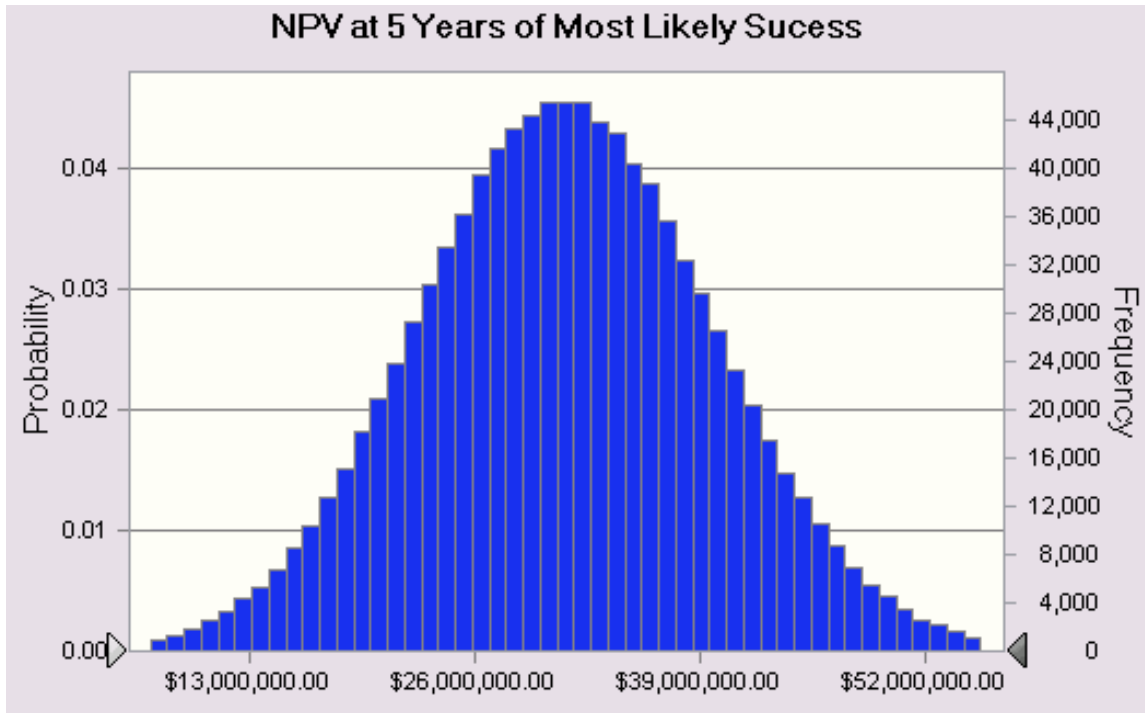


Figure 31: NPV Distribution at 5 Years of Most Probable Success

Figure 32 illustrates the NPV of the possible successful pathways through FDA testing. Four distinct modules were constructed through the FDA approval process, and there are two sub-sets within each module, one sub-set represents the passing of FDA testing with negligible difference in the side effects observed, while the other sub-set represents a reduction of the side effects using the delivery technology. A decrease in the side effects using the delivery technology was assumed to increase the demand for the delivery system by 25%; therefore, increased sales observed were in the sub-set of each module. Module 1 refers to the scenario where the micelle crosses the blood-brain barrier with the MAb acting as a vector with a larger reduction in the size of the tumor, and contains successful scenarios 1 and 2; successful scenario 1 represents a slight reduction in side effects, and successful scenario 2 represents a large reduction in side effects. Module 2 refers to the scenario where the micelle crosses the blood-brain barrier with the addition of a vector for transcytosis, resulting in a larger reduction in the size of the tumor than cur-

rent treatments, and contains successful scenarios 3 and 4; successful scenario 3 represents a slight reduction in side effects, and successful scenario 4 represents a large reduction in side effects. Module 3 refers to the scenario where the micelle crosses the blood-brain barrier with the MAb acting as a vector with a slight improvement in drug efficacy, and contains successful scenarios 5 and 6; successful scenario 5 represents a negligible reduction in side effects, and successful scenario 6 represents a minor reduction in side effects. Module 4 refers to the scenario where the micelle crosses the blood-brain barrier with the addition of a vector used for transcytosis with a slight improvement in drug efficacy, and contains successful scenarios 7 and 8; successful scenario 7 represents a negligible reduction in side effects, and successful scenario 8 represents a minor reduction in side effects.

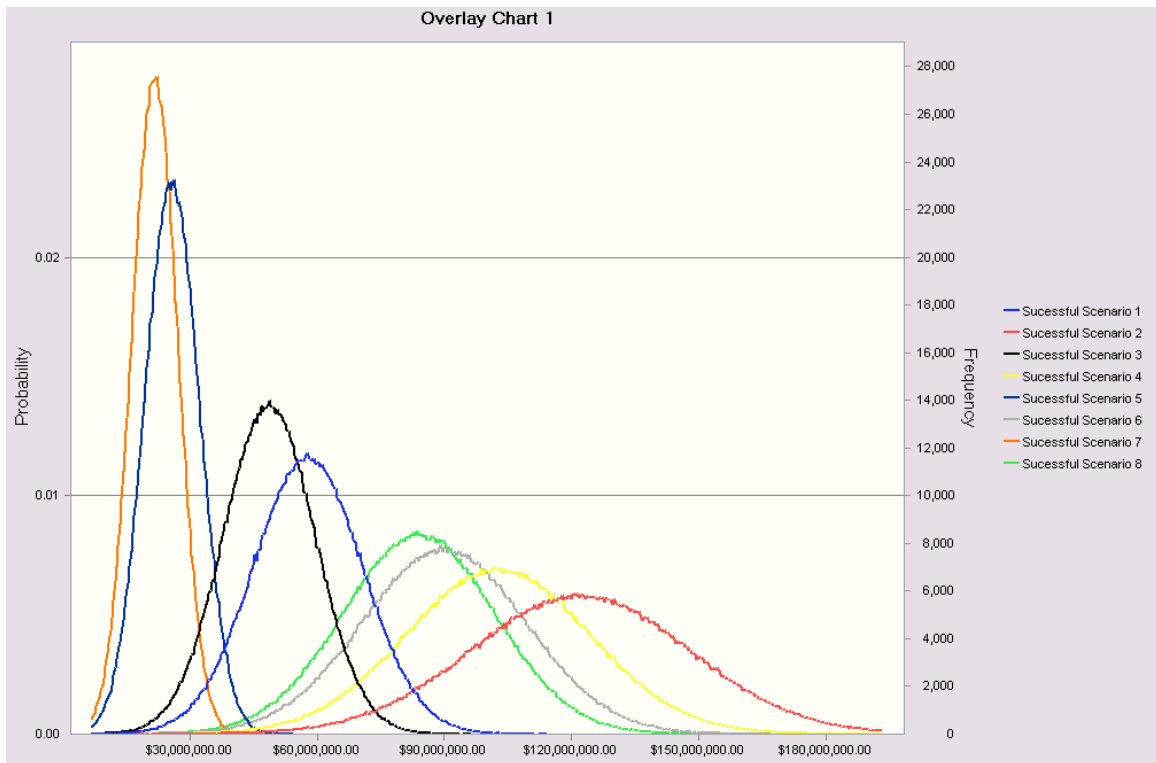


Figure 32: NPV Distributions for Successful Pathways

Figures 33 to 37 illustrate the individual modules, with the separation indicating an increase in NPV due to reduced side effects and improved tumor reduction.

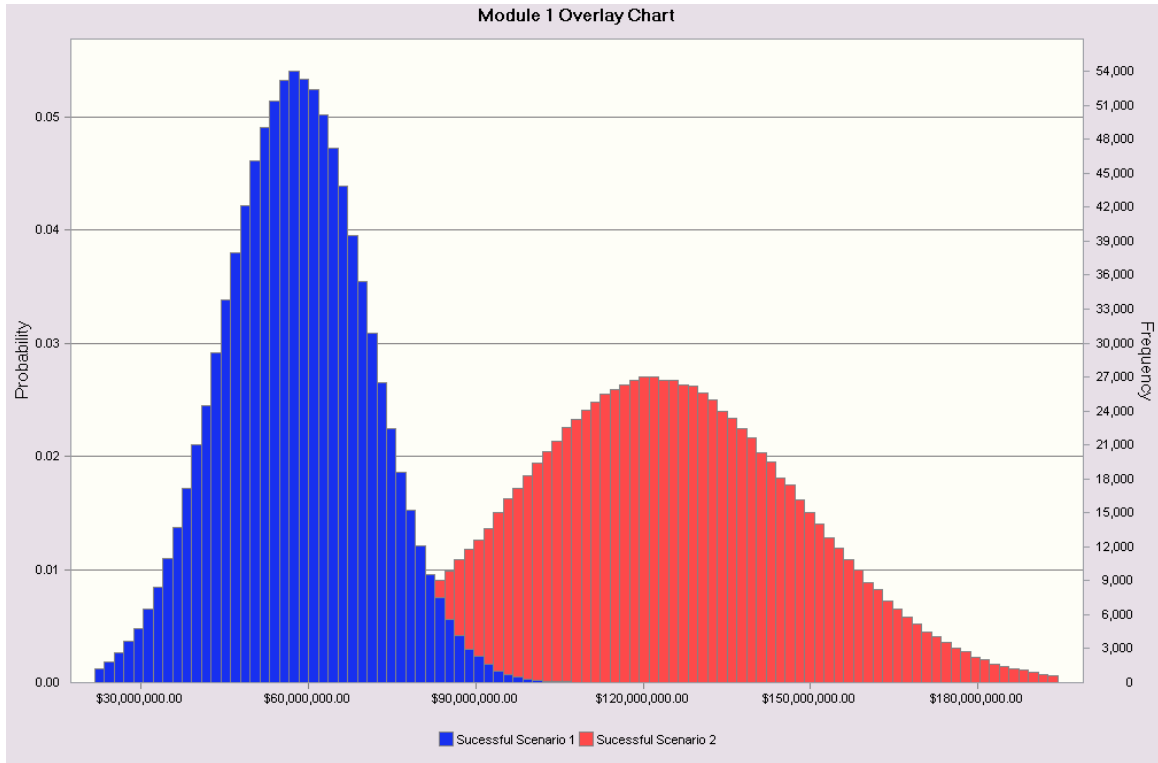


Figure 33: Module 1 NPV Distribution

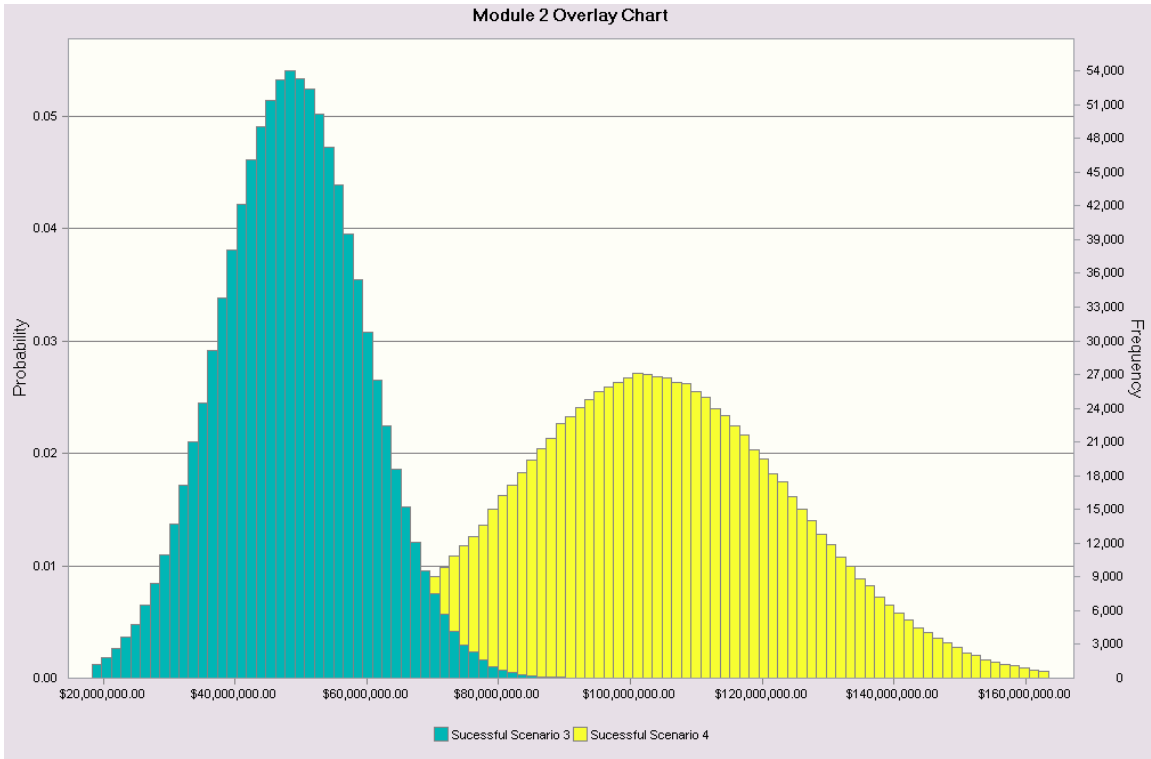


Figure 34: Module 2 NPV Distribution

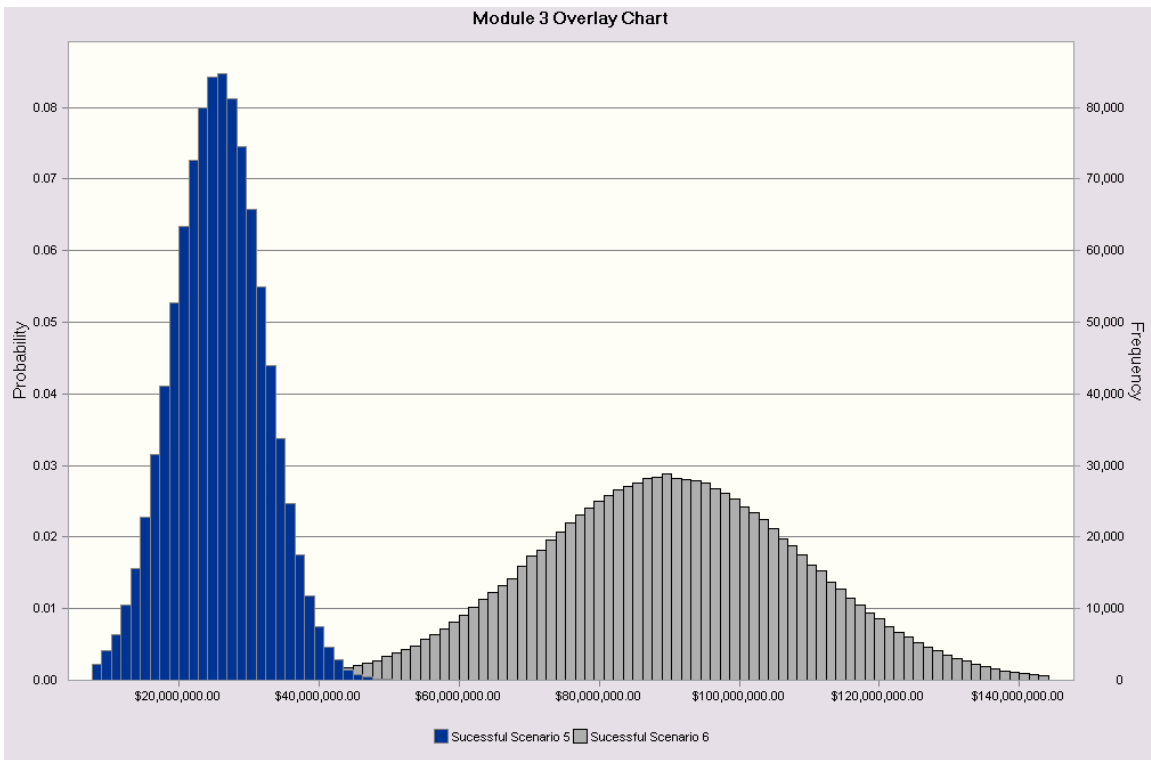


Figure 35: Module 3 NPV Distribution

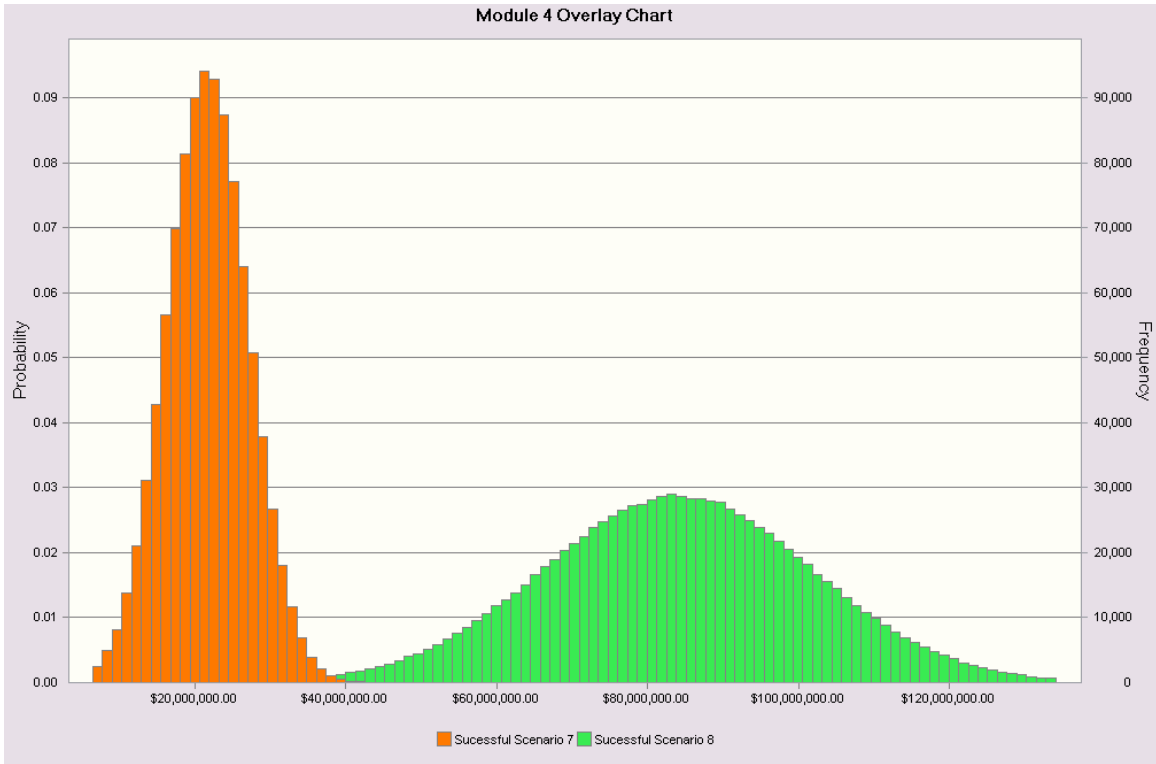


Figure 36: Module 4 NPV Distribution

10. Conclusions

In conclusion, the technical and financial analyses performed by CCKK Drug Delivery Technologies indicate that this project has a reasonable probability of success in terms of the biotechnology industry. Potential losses associated with this project are minimal in comparison to the potential gains, and the expected NPV indicates a high profitability. As such, CCKK Drug Delivery Technologies recommends that commercialization begin as soon as possible.

11. References

1. Janeway, Charles A., et al. Immunobiology. 5th ed. New York: Garland Publishing, 2001.
2. Stevens, Glen. Brain Tumors: Meningiomas and Gliomas. April 22, 2003. <http://www.clevelandclinicmeded.com/diseasemanagement/neurology/braintumor/braintumors.htm>
3. Cokgor, Ilkcan, et al. "Phase I Trial Results of Iodine-131-Labeled Antitenascin Monoclonal Antibody 81C6 Treatment of Patients With Newly Diagnosed Malignant Gliomas." Journal of Clinical Oncology. Vol. 18, No 22. 2000.
4. A Primer of Brain Tumors. American Brain Tumor Association. 1991. <<http://neurosurgery.mgh.harvard.edu/abta/primer.htm#Section6>>
5. Purves, Dale, et al. Neuroscience. 2nd ed. Sinauer Associate, Inc. 2001.
6. Pardridge, W.M. "Vector-mediated drug delivery to the brain." Advanced Drug Delivery Reviews. Vol. 36. April 1999.
7. Chiquet-Ehrismann, Ruth. *What Distinguishes Tenascin From Fibronectin?* The FASEB Journal. Vol. 4. June 1990.
8. Berg, Jeremy, et al. Biochemistry. W.H. Freeman and Co. 2002.
9. Torchilin, Vladimir P., et al. "Immunomicelles: Targeted pharmaceutical carriers for poorly soluble drugs." Proceeding of the National Academy of Sciences. May 13, 2003.
10. Bickel U., et al. "Delivery of Peptides and Proteins through the Blood Brain Barrier." Advanced Drug Delivery Review. Vol. 46. March 1, 2001.
11. Kansas State University Online Newspaper – Firm Explores Nanoparticle Uses <http://www.kstatecollegian.com/issues/v104/sp/n084/news/citygov.nanoparts.html>
12. Reszka, R., et. al., "Body Distribution of Free, Liposomal and Nanoparticle-Associated Mitoxantrone in B16-Melanoma-Bearing Mice", Journal of Pharmacology and Experimental Therapeutics, vol. 280, no. 1, 1997, p. 232-237
13. Ramge, Peter, et. al. "Polysorbate-80 coating enhances uptake of polybutylcyanoacrylate (PBCA)-nanoparticles by human and bovine primary brain capillary endothelial cells" European Journal of Neuroscience, Vol. 12, p.1931-1940, 2000
14. Zhang, ZR et. al., "Conjugation of Mitoxantrone-Loaded Nanospheres and Anti-C-erbB2 monoclonal antibodies", Yao Xue Xue Bao, Feb. 2001, vol. 36, issue 2, p. 151-154
15. Drugs Used to Treat Brain Tumors. Cancer Research UK. Januar 21, 2005. <<http://www.cancerhelp.org.uk/help/default.asp?page=5333>>
16. Harrison, Rodger G. et. al., Bioseparation Science and Engineering, Oxford University Press, New York, 2003
17. Zgurskaya, Helen, Biochemical Methods Class Lectures, Feb. 23rd and 25th
18. Torchilin, Vladimir, et al. *TAT peptide on the surface of liposomes affords their efficient intracellular delivery even at low temperature and in the presence of metabolic inhibitors*. National Academy of Sciences. 2001
19. Temodar (temozolomide) Capsules Product Information. Schering Corporation. Kenilworth, New Jersey. 2003.

20. Schmidt, Karl, et al. Volume Reconstruction Techniques Improve the Correlation Between Histological and *in vivo* Tumor Volume Measurements in Mouse Models of Human Gliomas. Journal of Neuro-Oncology. Kluwer Academic Publishers. 2004.
21. Strain: NU/J. The Jackson Laboratory. <<http://jaxmice.jax.org/jaxmice/cgi/jaxmicedb.cgi?objtype=pricedetail&stock=002019&dest=U>>
22. American Type Culture Collection. <<http://www.atcc.org/SearchCatalogs/Search.cfm>> 2005.
23. Walsh, Gary Ph.D. *Modern Antibody-Based Therapeutics.* Biopharm International. Volume 17, Number 12. pp. 18-25. Advanstar Communications Publication. December 2004.
24. Elder, Melissa. *Monoclonal Antibodies for Cancer.* Biopharm International. Volume 17, Number 11. pp 66. Advanstar Communications Publication. November 2004.
25. *Best Hospitals 2004 – Cancer.* US News. Online Source. <http://www.usnews.com/usnews/health/hosptl/rankings/specihqcanc.htm> 3/7/2005
26. *NIH Awards to all Intitutions by Rank 1-100, Fiscal Year 2003.* Online Source. <http://grants1.nih.gov/grants/award/trends/rnk03all1to100.html> 3/7/2005.
27. *NIH Research Grants Average Cost for Competing and Non-competing Awards Fiscal Years 1998-2003.* Online Source <http://grants1.nih.gov/grants/award/research/RGAVG9803.htm> 3/7/2005
28. Keating, Rick. *Conceptualizing, Making, and Selling the Brand.* Biopharm International. Volume 18, Number 1. pp 48-49. Advanstar Communications Publication. January 2005.
29. Bickel, Ulrich, et al. *Pharmacologic effects in vivo in brain by vector-mediated peptide drug delivery.* Proceedings of the National Academy of Science. 1992.
30. Huwyler, Jorg, et al. *Brain Drug Delivery of Small Molecules Using Immunoliposomes.* Proceedings of the National Academy of Sciences. Neurobiology. 1996.
31. Temodar Product Information, Schering Corporation, 2003
32. *Blinkov, Samuil M., and Il-ya I. Glezer, eds.* The Human Brain in Figures and Tables: A Quantitative Handbook. Moscow: Basic Books, Inc, 1968
33. Freitas, Robert A., Jr. *Nanomedicine: Volume I: Basic Capabilities.* Georgetown, TX: Landes Bioscience, 1999
34. Welling, Peter G. *Pharmacokinetics Processes and Mathematics.* Washington, DC: ASC Monograph, 1986.
35. Makoid, Michael, et. al., *Basic Pharmacokinetics,* Creighton University <http://pharmacy.creighton.edu/pha443/pdf/mammillary%20models.pdf>
36. “Census Bureau Projects Nation's Population to Total 295 Million on New Year's Day” Online Source. 2005. <http://www.census.gov/Press-Release/www/releases/archives/population/003161.html>
37. Zhang, ZR et. al., “Conjugation of Mitoxantrone-Loaded Nanospheres and Anti-C-erbB 2 monoclonal antibodies”, Yao Xue Xue Bao, Feb. 2001, vol. 36, issue 2, p. 151-154

38. Alyautdin, Renad N., et. al., "Delivery of Loperamide Across the Blood-Brain Barrier with Polysorbate 80 Coated Polybutylcyanoacrylate Nanoparticles", *Pharmaceutical Research*, 1997, vol. 14, no. 3, p.325-328
39. Garcia, M. L., et. al., "Stability and ocular tolerance of cyclophosphamide-loaded nanospheres", *Journal of Microencapsulation*, March 2004, vol. 21, no. 2, p. 213-223
40. Ramge, Peter, et. al. "Polysorbate-80 coating enhances uptake of polybutylcyanoacrylate (PBCA)-nanoparticles by human and bovine primary brain capillary endothelial cells" *European Journal of Neuroscience*, Vol. 12, p.1931-1940, 2000

A1. Appendix 1

A1.1 Nanoparticles

Nanosphere/monoclonal antibody conjugates have been created by Dr. ZR Zhang and colleagues in China on the laboratory scale to deliver the toxin mitoxantrone to mammary cancer cells.³⁷ However, these have only been created and tested for antibody specificity, and no studies have been done using these conjugates to improve drug delivery *in vitro* or *in vivo*. They have also not yet been used to cross the blood-brain barrier and deliver cancer treatment toxins to brain tumors. However, polysorbate 80 coated nanoparticles have been shown to effectively cross the blood brain barrier in *in vitro* and *in vivo* studies.³⁸ There is no current work to bind a monoclonal antibody to polysorbate 80 coated nanoparticles. The attachment of a monoclonal antibody could make this a more effective cancer treatment drug delivery system by improving targeting of treatment to the tumor cells in the brain. Since monoclonal antibody 81C6 selectively binds to tenascin, which is present on an extracellular matrix protein common in gliomas cancer tissue, it would increase the amount of toxin delivered to the tumor and decrease the relative amount of toxin found throughout the body. If the nanoparticle is designed to break down and release the toxin between 36 and 72 hours after entering the body, it would allow for toxin delivery only to cancerous brain cells to which the antibody 81C6 binds, while the toxin containing nanoparticles would be mostly cleared out of the rest of the body before toxin release. However, designing a nanoparticle that would accomplish this goal proved very difficult based on the limited amount of information available about the diffusion of nanoparticles *in vivo* and on the problems with attaching the antibody to the nanoparticle. These problems are explained in detail in section three of this appendix.

A1.2 Production of Nanoparticles

Polybutylcyanoacrylate nanoparticles are prepared by emulsion polymerization. This involves the suspension of small globules of one liquid in a second liquid in which the first liquid is insoluble. The polymerization takes place in a mixture of water and ethanol, as the monomer butylcyanoacrylate is not soluble in this aqueous mixture. Poloxamer 188 and sodium sulfate were added as stabilizers. The toxin is added to this mixture at a concentration of 0.1% (m/v). Polybutylcyanoacrylate is then added dropwise to the solution. The mixture is then stirred for four hours at room temperature with a magnetic stirrer at 400 rpm. The solution pH is then adjusted to 6.0 +/- 0.5 with sodium hydroxide and stirred for another hour. The suspension is then filtered and the ethanol is removed under a vacuum until an aqueous suspension of nanoparticles remains. Mannitol is then added and the nanoparticles are freeze-dried for twenty four hours under vacuum. The product is then homogeneously dispersed in phosphate buffered saline (PBS) solution by ultrasonification, or the dispersion of product in the solution by sound wave energy. According to Renad N. Alyautdin and colleagues, polysorbate 80 is then added and the mixture is incubated for 30 minutes.³⁸

A1.3 Problems with Nanoparticle Treatment

- 1. Drug Release Time** – Polysorbate 80 coated nanoparticles are a very new idea, and little research has been done into the drug release time *in vivo*. According to Dr. M. L. Garcia and colleagues, an *in vitro* study of polymer nanoparticle degradation indicates that it could take weeks.³⁹ This would be too long for this treatment because the antibody would degrade and the nanoparticle would be washed out of the brain before drug release. However, this study is not indicative of the

drug release time *in vivo*. Enzymes and other biomolecules in the brain will interact with the nanoparticle and will likely cause it to degrade in chunks in the brain, which is a difficult process to effectively model. Therefore, extensive research will be necessary to determine the appropriate nanoparticle thickness, and the thickness may or may not have a significant impact on release time if there are significant interactions between the polysorbate 80 coating and the polybutylcyanoacrylate coating and enzymes in the brain. Thus it is not possible to predict with any certainty the likelihood of toxin release between 36 and 79 hours. This is the timeframe between the exit of the antibody from the body and from the exit of the antibody from the brain.

2. Particle Size – The nanoparticle must be small enough to cross the blood-brain barrier. Research results from Dr. Peter Rame and colleagues in Germany indicate that 450 nm is an appropriate maximum particle diameter for crossing the blood-brain barrier.⁴⁰ This would correspond to a particle radius of 225 nm. The total radius of the particle is modeled with the following equation:

$$r_T = r_{PBCA} + r_{PS}$$

where r_T is the total nanoparticle radius, r_{PBCA} is the radius of the polybutylcyanoacrylate nanoparticles before the addition of polysorbate 80, and r_{PS} is the thickness of the polysorbate coating. Research results indicate that r_{PBCA} is generally around 150 nm.⁴⁰ Therefore, the maximum polysorbate thickness possible is around 75 nm.

3. Antibody Attachment – The antibody must be attached to the polybutylcyanoacrylate nanoparticle shell, beneath the polysorbate 80 coating, in order for the antibody to effectively attach the nanoparticle to the tumor cells. The mechanism by which the antibody would attach to the polybutylcyanoacrylate is not easy to elucidate, as there are two possible locations where the antibody could bind. The nanoparticle could either bind at the amine group or the ester group as shown in the butylcyanoacrylate structure displayed below. However, these groups are both fairly stable and would be difficult to activate under known reaction conditions. Therefore, the antibody may not bind to the polybutylcyanoacrylate at all. There have been very few antibody-nanoparticle conjugates created and the mechanism of antibody attachment is not well elucidated in these examples. Therefore, it is very difficult to predict the likelihood of successful antibody attachment to the nanoparticle. For this reason, the antibody delivery design was abandoned in favor of the micelle design.

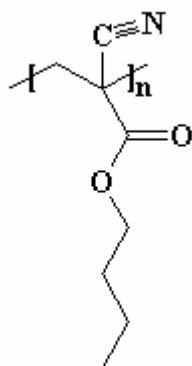


Figure 37: Structure of Polybutylcyanoacrylate
Image courtesy of <http://www.psrc.usm.edu/macrog/pca.htm>

A1.4 Pre-FDA Testing of Nanoshell Delivery Mechanism

Figure 38 illustrates the research and development phase of the nanoshell encapsulation. There are four major behaviors of the nanoshell and antibody that are being investigated in this section. The first aspect being investigated is release time of the nanoshell and accompanying toxin. If the nanoshell delivery mechanism passes this stage with a release time of 36-79 hours, then the project will progress on to BBB crossing testing. In this phase of the testing if the MAb does not allow the nanoshell to cross the BBB, then the project will fail. If the BBB can be crossed by the nanoshell and antibody, the testing will then proceed to the next stage. The third stage of testing is to investigate the effects the nanoshell and accompanying toxin will have on the parts of the body which are not cancerous. This includes all areas which have the binding site specific to the antibody as well as any areas of the body which are affected by the chemotherapy toxin. This is a comparison of the side effects of the chemotherapy alone to the nanoshell delivery system. If the effects on non-cancerous areas of the body are roughly equivalent to or less than the chemotherapy alone, then the final stage of Pre-FDA testing will be entered. If the effects on non-cancerous areas of the body is more than the current chemotherapy then the project will fail. The final stage of testing is to observe the effective reduction of the tumor. In this case it is necessary to observe a reduction of the tumor that is at least as much as the chemotherapy alone. If there is a negligible difference in the reduction of the tumor using the nanoshell as compared to the chemotherapy alone then it becomes necessary to evaluate the extent of the side effects. If the side effects are less than the current chemotherapy when using the nanoshell, the project still has merit and should proceed; if the side effects are negligibly reduced then the project will fail.

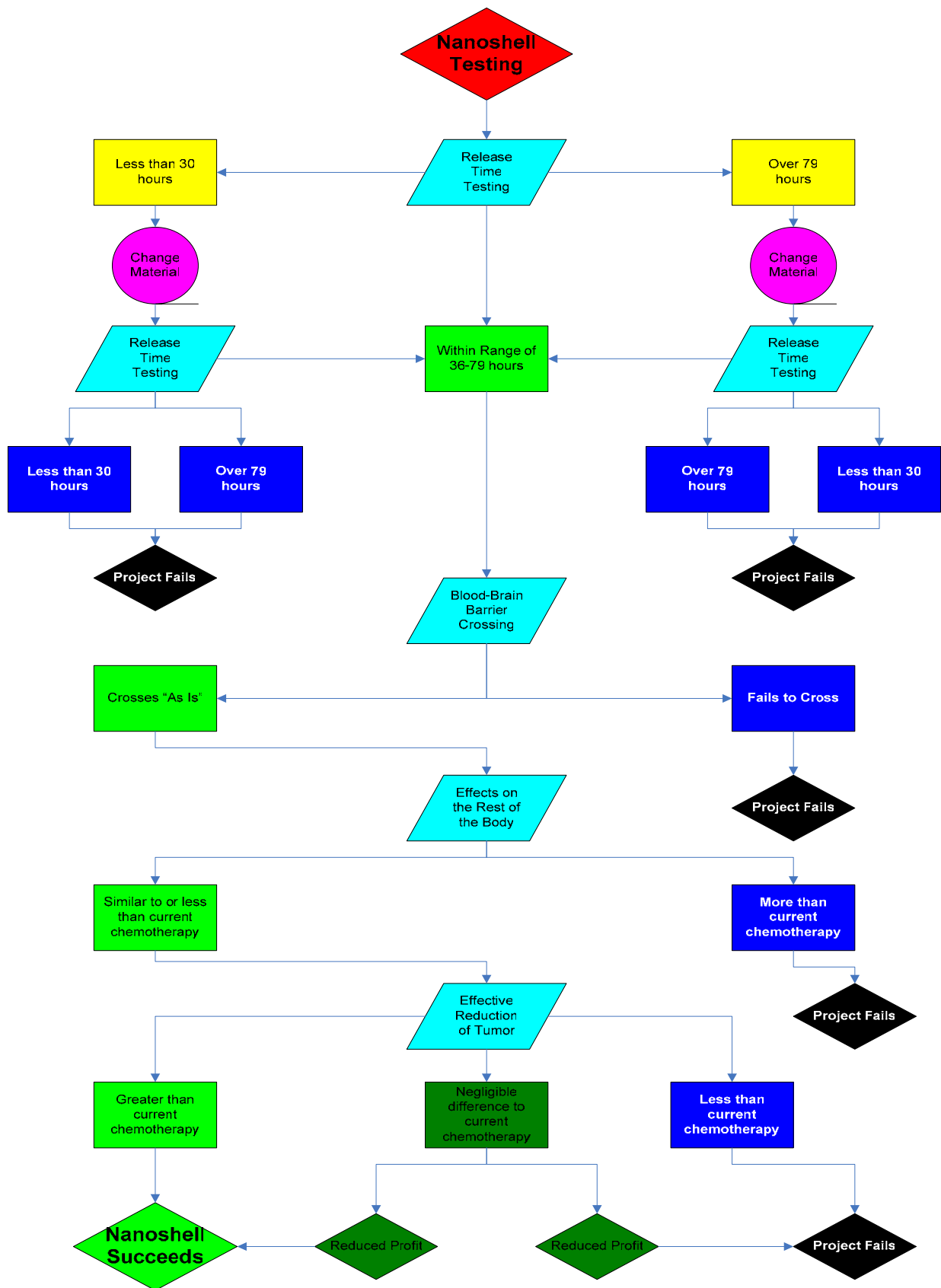


Figure 38: Pre-FDA Testing of Nanoshell Flowchart

A2. Appendix 2

A2.1 Pharmacokinetic Parameter Derivation

For the purposes of modeling the changing concentration with time during the alpha phase of the brain elimination model,³⁴ the body and the half of the brain of interest were modeled as two well-mixed vessels with blood continually circulating between them. The volume of the blood in the body has been determined to be 5 liters, and the blood circulates throughout the body every minute. As the flow through the half of the brain is 370 mL/min, it is assumed that the volume of blood contained in the brain is 370 mL. The flow rate between the brain and the body is assumed to be equal to the flow rate in the internal carotid artery, or 370 mL/min. The model is diagrammed below.

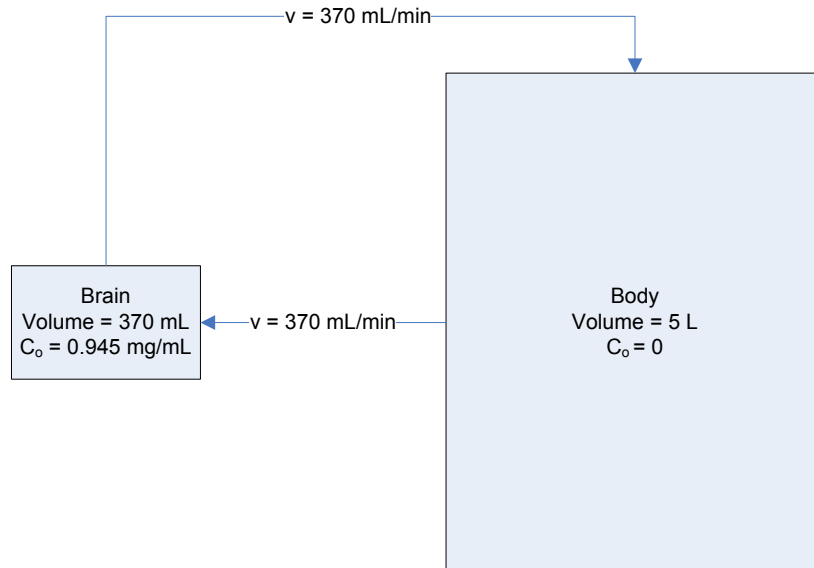


Figure 39: Two Compartment Model Diagram

In order to determine the change in concentration in the brain with time, differential mass balances were derived for each compartment of the model, shown as follows:

$$\frac{dM_{brain}}{dt} = \left(\frac{dC_{brain}}{dt} \right) V_{brain} = M_{in} - M_{out} = v(C_{body} - C_{brain})$$

$$\frac{dM_{body}}{dt} = \left(\frac{dC_{body}}{dt} \right) V_{body} = M_{in} - M_{out} = v(C_{brain} - C_{body})$$

where M is the mass of drug in a given compartment, C is the concentration in the compartment, V is the volume of blood in the compartment, v is the flow rate between the two compartments, and t is time.

In order to solve the two equations, it was assumed that

$$\left(\frac{dC}{dt} \right) \approx \left(\frac{\Delta C}{\Delta t} \right)$$

$$\Delta C \approx \frac{v\Delta t}{V} (C_{in} - C_{out})$$

Solving for the change in concentration for each compartment of the model, a series of small increments of time were used with the known volumes and volumetric flow rates to plot the change of concentration in both the brain and the body with time. The initial concentration for the body was assumed to be zero, and the initial concentration was determined to be 0.945 mg/mL, as calculated from the injection model presented in Section 7.3. The results can be seen in Figure 19.

From this plot, the final equilibrium concentration within the brain and body was taken to be the point at which the concentrations of the two compartments were equal, determined to be 0.067 mg/mL. The total time for equilibration, effectively the duration of the elimination phase, was found to be approximately 6 minutes. From the plot, the time for the concentration in the brain to change by half, the half-life of the phase, was determined to be 0.625 minutes.

From this calculated half-life for the alpha phase, and assuming that the half-life of the beta phase is equal to that calculated in the oral model, the α and β parameters were determined from the following relationships:³⁴

$$\alpha = \frac{\ln(2)}{(t_{1/2})_{\alpha}} \qquad \beta = \frac{\ln(2)}{(t_{1/2})_{\beta}}$$

The parameter A_1 is the y-intercept of the redistribution phase, shown in Figure 18.³⁴ This value was determined by taking the amount of drug not delivered to the tumor (calculated from the injection model by assuming a mean tumor volume of 1.25 cc) and dividing the mass of drug by the volume of blood contained in the brain, 370 mL. The parameter B_1 is the theoretical y-intercept of the elimination phase, also shown in Figure 18.³⁴ This was determined by taking the initial amount of drug in the body, also assumed to be the amount of drug not delivered to the tumor upon initial injection) and dividing by the total amount of blood contained within the body, 5000 mL. The values calculated for α , β , A_1 , and B_1 can be found in Table 1.

These parameters are related to the rate constant describing the transfer of drug from the body to the brain, k_{21} , by the following relationships:³⁴

$$A_1 = \frac{D(\alpha - k_{21})}{V_1(\alpha - \beta)} \qquad B_1 = \frac{D(k_{21} - \beta)}{V_1(\alpha - \beta)}$$

Where D is the dosage of injected drug, assumed to be 350 mg, and V_1 is the apparent volume of unchanged drug distribution in compartment 1. The value of V_1 is calculated by the following equation:

$$V_1 = \frac{Dose}{A_1 + B_1} = \frac{350 \text{ mg}}{(0.945 + 0.07) \text{ mg} / \text{mL}} = 345 \text{ mL}$$

Using these values, the value of k_{21} was calculated and presented in Table 1.

Additional relationships for the pharmacokinetic rate constants are as follows:³⁴

$$\alpha\beta = k_{10}k_{21}$$

$$\alpha + \beta = k_{12} + k_{10} + k_{21}$$

From these equations and the calculated parameters presented above, values for the kinetic rate constants describing the distribution and elimination of the drug from the brain were calculated and can be found in Table 1.

A3. Appendix 3

A3.1 NPV Distributions of Each Successful Scenario

